DOI:10.14753/SE.2012.1723

New Echocardiographic Techniques in Rare Cardiological Disorders

Doctoral Thesis

Gabriella Veress MD

Semmelweis University
Doctoral School of Basic Medicine

Supervisor
Béla Merkely MD, DSc, Professor of Medicine

Official Reviewers
Lívia Jánoskúti MD, PhD
Albert Varga MD, PhD, Professor of Medicine

Head of Examination Committee
Zoltán Szabó, MD, PhD, Professor of Medicine

Members of Examination Committee
József Borbola, MD, PhD, Professor of Medicine
András Zsáry MD, PhD

Budapest
2011

DOI:10.14753/SE.2012.1723

1 Table of contents

DOI:10.14753/SE.2012.1723

2 Abbreviations

ε: strain

2D: two-dimensional

A: late diastolic velocity of the mitral wave

a': late diastolic annulus velocity

ACC: American College of Cardiology

AF: atrial fibrillation

AHA: American Heart Association

ASE: American Society of Echocardiography

BMI: body mass index

BS/BL: basal septum/basal lateral

BSA: body surface area

CA: cardiac amyloidosis

CMR: cardiac magnetic resonance

cMR: cine magnetic resonance

COPD: chronic pulmonary obstructive disease

CP: constrictive pericarditis

CRT-D: cardiac resynchronization therapy defibrillator

CT: computer tomography

DM: diabetes mellitus

DMI: Doppler myocardial imaging

dMV-E: early diastolic peak value for myocardial velocity

dSR-E: early diastolic strain rate

DT: deceleration time

DVT: deep vein thrombosis

E: early diastolic wave of mitral inflow

e': early diastolic annulus velocity

EF: ejection fraction

EMB: endomyocardial biopsy

FPS: frame per second

Fr: french

HL: hyperlipidemia
HR: heart rate
HT: hypertension
HTX: heart transplantation
ICD: intracardiac defibrillator
IJ: internal jugular
iLVNC: isolated left ventricular non-compaction
iv.: intravenous
IVRT: isovolumetric relaxation time
JVP: jugular venous pressure
LA: left atrium
LAVI: left atrial volume index
LMWH: low-molecular weight heparin
LV rot: left ventricular rotation
LV tor: left ventricular torsion
LV: left ventricle
LVAD: left ventricular assist device
LVEDD: left ventricular end-diastolic diameter
LVEF: left ventricular ejection fraction
LVESD: left ventricular end-systolic diameter
MM: mycophenolate mofetil
MS/ML: mid septum/mid lateral
MV: mitral valve
MVG: myocardial velocity gradient
NCCM: non-compact cardiomyopathy
PWTDI: pulse wave tissue Doppler imaging
NS: non-significant
PPM: permanent pacemaker
PW: posterior wall
RA: right atrium
RCM: restrictive cardiomyopathy
ROC: receiver-operating characteristics

DOI:10.14753/SE.2012.1723

RV: right ventricle
RVEDP: right ventricular end-diastolic pressure
RVESP: right ventricular end-systolic pressure
s': systolic annulus velocity
sD: systolic displacement
SMI: speckle myocardial imaging
sMV: systolic peak value for myocardial velocity
SRI: strain rate imaging
sS: systolic strain
sSR: systolic strain rate
STE: speckle tracking echocardiography
SVC: superior vena cava
vs.: versus
TDI: tissue Doppler imaging
TEE: transesophageal echocardiography
TIA: transient ischaemic attack
TTE: transthoracic echocardiography
TV: tricuspid valve

DOI:10.14753/SE.2012.1723

3 Introduction

The new echocardiographic techniques characterize the mechanics of myocardial contraction and relaxation precisely and have been applied in numerous cardiac disorders.

There is no substantial amount of information available in cardiac tissue Doppler analysis and deformation imaging, as in strain and strain rate imaging by speckle tracking imaging in rare cardiologic disorders, such as constrictive pericarditis (CP), restrictive cardiomyopathy (RCM) and isolated noncompact cardiomyopathy (iLVNC). Our studies were focusing on better understanding of the functional and pathophysiological changes in the heart within the above referenced disorders by new echocardiographic techniques. In addition, we have examined the additional benefit of echocardiography guided endomyocardial biopsy (EMB) in lieu of fluoroscopic guidance alone during the procedure relative to the recognition of hitherto unreported sequels.

3.1 Rare cardiological disorders

3.1.1 Constrictive pericarditis

CP is frequently difficult to diagnose even after comprehensive evaluation, and often not considered in the differential diagnosis of patients with heart failure. Echocardiography has made a significant contribution to the accurate and increasing diagnosis of CP and is the imaging modality of choice for the initial evaluation of patients with suspected CP.

The echocardiographic diagnosis of CP was originally based on M-mode echocardiography findings and subsequently on 2D echocardiography and Doppler hemodynamics.[1] M-mode provides useful information in CP, although not specifically diagnostic for the disease. One of the several findings that may be seen on M-mode is thickened pericardium. While 15-20% of CP patients had normal pericardium in a study by Talreja[2], mildly increased pericardial thickness can be often missed or often false positive results can be obtained if gain is set too high. Abrupt posterior motion of the interventricular septum with inspiration in early diastole can also be seen, which is the

consequence of the underfilling of the ventricle due to decreased pulmonary vein-left atrial gradient with inspiration.[3] Further signs on M-mode are flat posterior LV wall motion in mid-diastole[4] and ventricular septal notch in early diastole due to transient reversal of ventricular septal transmural pressure at that time in the cardiac cycle.[5, 6] Left atrial enlargement, premature opening of the pulmonary valve caused by the rapid early diastolic filling of the right ventricle[7] and abnormalities in posterior aortic root motion, such as sharp downward motion of the posterior aortic root in early diastole can also be observed.

The role of 2D echocardiography initially was to rule out other causes of right heart failure such as pulmonary hypertension, unexpected LV dysfunction or valvular disease.[8] In CP normal ventricular dimensions can usually be seen on 2D with normal systolic function, where ejection fraction is typically preserved, although may be impaired in mixed constrictive-restrictive disease. Pericardial thickness and calcification can be assessed to some extent. Transesophageal echocardiography (TEE) is superior to transthoracic echocardiography (TTE) in measuring the pericardial thickness and has an excellent correlation with cardiac tomography (CT).[9] The 2003 ACC/AHA/ASE task force gave a class IIb recommendation to TEE assessment of pericardial thickness to support the diagnosis for CP.[10] Abnormal ventricular septal motion/early diastolic septal bounce resulting from exaggerated ventricular interaction can be frequently observed. Elevated right atrial pressures are reflected by a dilated inferior vena cava with minimal or no respiratory variation in its diameter. If present, pericardial or pleural effusion can be identified. Further signs can be observed by 2D echocardiography include displacement of the interatrial septum towards the left atrium (LA) during inspiration, some dilatation of the atria, especially the LA, and an abnormal contour between the posterior LV and the LA posterior walls.[11]

Doppler echocardiography is essential in CP diagnosis showing early increased diastolic filling velocity (E) followed by rapid deceleration leading to a short filling period with mitral E wave typically being <160 ms. In addition, Hatle and Oh described the characteristic mitral inflow respiratory variation exceeding 25% in Doppler flow velocities in CP patients that are not present in patients with RCM. [12, 13] (Figure 1) The major factor responsible for this phenomenon is the dissociation of intrathoracic and intracardiac pressures with respiration.

DOI:10.14753/SE.2012.1723

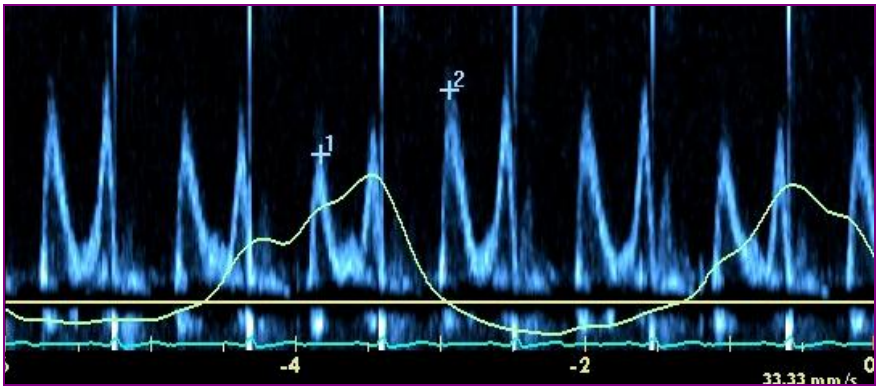

Figure 1. Mitral inflow in constrictive pericarditis. Characteristic respiratory variation > 25% of mitral E wave (1 vs.2).

Normally, with inspiration the intrathoracic pressure decreases approximately to the same extent as the intracardiac pressure therefore the pressure gradient remains quasi the same. In CP with inspiration, the intrathoracic pressure declination, due to pericardial isolation is not fully transferred to the intracardiac pressure. Consequently, the pressure gradient is lowered and LV diastolic filling is reduced. As in CP the cardiac volume is relatively fixed, this is coupled with a simultaneous RV diastolic filling increase, resulting in left interventricular septum shift. The opposite change occurs with expiration. [13]

This respiratory variation in transmitral flow is not present in RCM or in normal subjects but can be observed in patients with chronic obstructive airway disease (COPD).[14] For differentiating CP from COPD by Doppler echocardiography superior vena cava (SVC) flow velocities can be recorded. In COPD there is a marked increase in systolic forward flow velocity during inspiration, which is not seen in CP. In CP the SVC diastolic flow velocity exceeds systolic flow velocity and there is little respiratory variation in systolic flow velocity.[15]

DOI:10.14753/SE.2012.1723

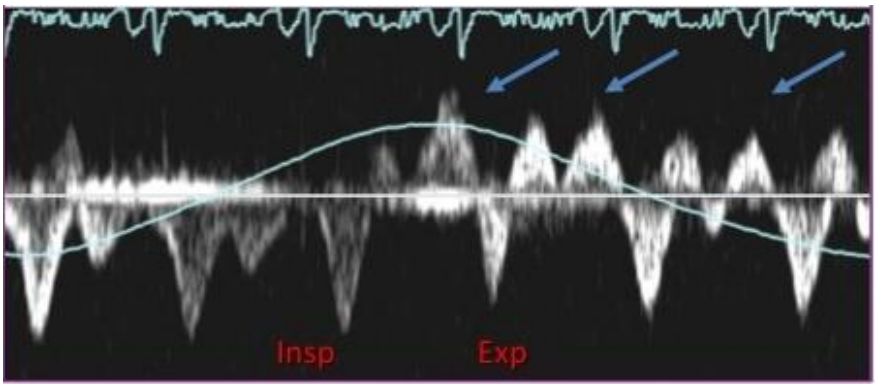

Figure 2. Hepatic vein flow in constrictive pericarditis. Arrows: expiratory, diastolic flow reversal. Insp: inspiration, Exp: expiration.

In addition, in a subset (20%) of CP patients the typical respiratory variation of mitral E velocity may not be present, which can be due to LA pressure increase or to mixed constrictive-restrictive pathophysiology.[13] Oh et al proposed in this group of patients additional echocardiographic tests to reduce preload (by head-up tilt, upright position, or diuresis) that may help unmask or enhance respiratory variation on transmitral Doppler flow.[16] Atrial fibrillation makes the interpretation of respiratory variation in Doppler velocities difficult, however with meticulous analysis of a longer Doppler strip chart makes the interpretation of underlying hemodynamic mechanism possible.[13] Doppler interrogation of the hepatic vein can also be useful for the diagnosis. The pulsed Doppler recording of hepatic venous flow (Figure 2) shows a diastolic flow reversal with expiration, reflecting the ventricular interaction and the dissociation of intracardiac and intrathoracic pressures. In mixed constrictive-restrictive cases both expiratory and inspiratory flow reversal can be seen.[13]

With the help of TEE, pulmonary venous flow can be studied. A peak diastolic flow velocity fall of > 40% on inspiration and a systolic/diastolic flow ratio < 0.65 in inspiration demarcates CP from RCM.[17] The respiratory variation in pulmonary venous flow is even more pronounced than in mitral inflow[18] (Figure 3).

The assessment of myocardial contraction and relaxation using Doppler myocardial velocity gradient (MVG) at the LV posterior wall may be another method distinguishing CP from RCM. MVG quantifies the spatial distribution of intramural velocities across the myocardium.[19] It was shown that MVG was lower in RCM patients compared with

both CP patients and normal controls during ventricular ejection and rapid ventricular filling, measured at the left ventricular posterior wall.[20]

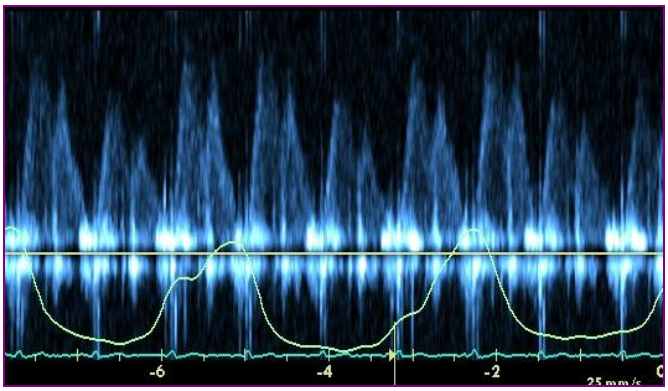

Figure 3. Pulmonary vein flow in constrictive pericarditis. Marked respiratory change in pulmonary venous flow.

TDI offers a quantitative measurement of regional and global myocardial tissue function. In particular, the assessment of longitudinal mitral annular motion provides an accurate estimate of global LV function[21] and it has further facilitated the detection of CP. Since the mechanoelastic properties of the myocardium are preserved in CP, the longitudinal mitral annular velocities remain normal or can be exaggerated as lateral expansion in CP is limited.

Garcia et al were the first to report that measurement of longitudinal axis expansion by TDI provided a clinically useful distinction between CP and RCM.[22] Rajagopalan et al showed that a peak e' velocity ≥ 8 cm/s could discriminate between the entities CP and RCM with high sensitivity (89%) and specificity (100%).[23] Studies by Ha et al and by Sohn et al recommended that e' velocity can provide a helpful diagnostic indicator and should be measured routinely in the evaluation of heart failure or suspected CP.[24, 25] Ha et al recommended the same 8 cm/s cut off value for CP diagnosis where e' velocity is equal or greater than 8 cm/s, with 95% sensitivity and 96% specificity.[24] Ha et al also evaluated the role of TDI in the diagnosis of CP in patients without diagnostic respiratory variation of transmitral early diastolic filling velocity. It was confirmed that e' velocity was well-preserved independent of any respiratory variation in mitral inflow velocities.[26] Other studies suggested that e' should be used with caution if CP is combined with myocardial diseases, extensive annular calcification or segmental non-uniform myocardial velocities.[27, 28, 29] It has been shown by Choi et al that the addition

of extra parameters to the e' velocities such as measurement of s' velocities and the time difference between onset of mitral inflow and onset of e' increases sensitivity and provide additional information to e' for the differentiation of CP from RCM.[30]

Several investigators have shown that E/e' ratio correlates well with LV filling pressure.[31, 32] E/e' >15 identifies increased LV filling pressure while E/e' <8 describes normal filling pressure. Ha introduced the concept of 'annulus paradoxus', which describes the paradoxical behavior of the mitral annulus in CP.[33] He found that an inverse relationship exists between E/e' and LV filling pressure, which can be explained by the fact that in CP the mitral annulus has an exaggerated longitudinal motion leading to an increase in e', despite high filling pressures.

In normal subjects, the mitral lateral annulus e' velocity is higher than the medial annulus e' velocity.[34] Reuss et al identified the reversal of the normal relationship of mitral lateral e' and medial e' velocities in CP, where mitral lateral e' velocity is lower than medial e' velocity, therefore lateral/medial e' ratio is inverted and called „annulus reversus".[35] This finding is based on the tethering of the adjacent fibrotic and scarred pericardium, which influences the lateral mitral annulus in patients with CP. In a patient with preserved mitral e' velocities (> 8 cm/sec) and a low E/e'ratio (< 8) with high LV filling pressure, the recognition of „annulus reversus" should alert to the diagnosis of CP.

In general, TDI offers incremental diagnostic information to M-mode, 2D echo and transmitral flow Doppler for detecting constrictive physiology, with a reported sensitivity and specificity of 88.8% and 94.8%, respectively.[27]

Kim JS and al examined the medial annular velocities in patients with CP after pericardiectomy in 16 patients and found that e' decreased significantly after pericardiectomy.[36] However, there is no substantive data on mitral annulus systolic velocity and tricuspid annulus velocity in CP and no data on the effect of pericardiectomy on these annular velocities.

3.1.2 Restrictive cardiomyopathy

The clinical and hemodynamic profiles of restriction (myocardial diastolic heart failure) and constriction (pericardial diastolic heart failure) are similar, even though their pathophysiologic mechanisms are distinctly different. Both are characterized by limited

or restricted diastolic filling with relatively preserved global systolic function. Diastolic dysfunction in RCM is the result of a stiff and noncompliant ventricular myocardium, whereas in CP diastolic dysfunction is related to a thickened or noncompliant pericardium. Both disease process limit diastolic filling and result in diastolic heart failure.

Despite the distinct difference in pathophysiologic mechanisms of restriction and constriction, the hemodynamic variables of these two conditions overlap considerably. Increased atrial pressures, equalization of end diastolic pressures, and dip-and-plateau (or square root sign) of the ventricular diastolic pressure recording have been widely considered as the hemodynamic features typical of CP.[37] Hemodynamic pressure tracings with almost identical characteristics can be obtained from patients who have either constriction or RCM.[38] While the echocardiographic features of amyloid infiltration of the heart are fairly characteristic in the advanced stages of the disease, early cardiac infiltration may produce a mixed and confusing picture. Echocardiographic features of amyloid infiltration of the heart in advanced stages are as follows:

- increased LV/RV wall thickness,
- enlarged LA,
- valve thickening,
- usually mild mitral regurgitation,
- thickened atrial septum,
- E/A ratio >1 and
- pericardial effusion.

Making the distinction between CP and RCM is a diagnostic challenge. The diagnosis of CP is clinically important for a timely treatment but often very challenging even after comprehensive evaluation using various cardiovascular imaging and hemodynamic studies.

Strain and strain rate are measures of deformation that are basic descriptors of both the nature and function of cardiac tissue. 2D speckle tracking echocardiography (STE) is a new technique, based on frame-by-frame tracking of tiny echo-dense speckles within the myocardium and subsequent measurement of left ventricular deformation.[39, 40]

Mitral septal annular velocity is usually increased in patients with CP and higher than the lateral annular velocity.[24, 26] We hypothesized that the longitudinal strain of the lateral wall that is in contact with diseased pericardium is lower than that of the medial segments in CP.

3.1.3 Acute thrombus formation related to endomyocardial biopsy

Endomyocardial biopsy is currently the technique most often used in the diagnosis of cardiac transplant rejection and it is the standard method for evaluating infiltrative cardiac lesions, cardiomyopathies and myocarditis.[41] It is generally considered a safe procedure but is associated with recognized significant complications related to venous cannulation, arrhythmias and conduction abnormalities as well as inadvertent trauma to cardiac structures such as the tricuspid valve, tricuspid valve apparatus and right ventricular free wall.[42] Endomyocardial biopsy is usually performed under fluoroscopic guidance. However, adjunctive echocardiography is increasingly used since it permits precise positioning of the bioptome, minimizing the risk of complications. In addition, echocardiography facilitates prompt recognition and treatment of complications if these do occur.[43]

3.1.4 Non-compact cardiomyopathy

NCCM is rare, unclassified, congenital cardiomyopathy due to embryogenic arrest of compaction[44], previously described as persistent intramyocardial sinusoids. NCCM is genetically heterogenous condition with both familial and sporadic forms described.[45] Because of the significant potential for cardiovascular complications, early recognition is essential. It is characterized by segmental thickening of the LV wall consisting of two layers: a thin compacted epicardial layer and a thickened endocardial layer with marked trabeculations and deep intratrabecular recesses. Ventricular noncompaction is often associated with other congenital cardiac malformations, such as obstruction of the left and right ventricular outflow tracts, complex congenital malformations and coronary anomalies.[46, 47, 48]

The clinical manifestations of noncompacted cardiomyopathy are variable. Patients may be asymptomatic or may demonstrate evidence of congestive heart failure, arrhythmias or systemic emboli.[44, 49, 50, 51]

Application of the echocardiographic diagnostic criteria for left ventricular non-compaction as postulated by Jenni[52] et al together with advances in cardiac imaging techniques have enhanced awareness and diagnosis of left ventricular noncompaction. The four morphologic criteria for echocardiographic diagnosis are the followings:

- lack of coexisting cardiovascular abnormalities,
- segmental LV wall thickening with a thin compacted epicardial layer and a thicker noncompacted endocardial layer,
- an end-systolic noncompacted-to-compacted myocardial ratio > 2.0 and
- the presence of color Doppler flow within the deep intertrabecular recesses.

Patients with these morphologic features may present with normal or abnormal LV function as assessed by EF. Although, iLVNC is included in the 2006 World Health Organization classification of cardiomyopathies, however, its etiology, pathogenesis, diagnosis, and management have to be further defined.

3.2 New echocardiographic techniques

Echocardiography has been a pillar of modern cardiology practice, with several decades of increasing utilization as international practice guidelines progressively expanded the number and type of indications for which this diagnostic modality was approved.[53] From the perspective of the single cardiology patient, the standard echocardiogram has provided a comprehensive and rapid assessment of their heart's unique structure and function, and played a critical role in allowing each person's cardiology care plan to be successfully individualized. Nevertheless, looking towards the future, we can identify several new aspects of echocardiographic techniques that must be tested and, where successful, integrated into recommended practice.

In particular, during recent years remarkable progress has been made in cardiac tissue Doppler analysis, strain and strain rate imaging by speckle tracking imaging. They characterize the mechanics of myocardial contraction and relaxation (deformation imaging) more precisely and find applications in many cardiac pathologies.[54] Determination of myocardial function is vital for the clinical evaluation of cardiovascular diseases. It not only helps to establish a diagnosis, but often can provide

important prognostic and management information that is invaluable in a variety of cardiac diseases. Early detection of abnormalities is crucial and may often influence treatments and establish prognosis.

3.1.5 Tissue Doppler echocardiography: principles and applications

TDI is a novel use of ultrasound to image the motion of tissue with Doppler echocardiography. It is a robust and reproducible echocardiographic tool, which has permitted a quantitative assessment of both global and regional function and timing of myocardial events.[55, 56]

Tissue Doppler velocity estimation is based on the same principles as pulsed-wave and color Doppler echocardiography for blood flow. To distinguish between signals originating from moving tissue and blood flow, a so-called wall filter is used, which is a high-pass filter used to image blood velocities or a low-pass filter used to display tissue velocities. While the intensity of the signals generated by the myocardium is higher than that generated by blood, blood velocity usually exceeds that of the myocardium.[57]

In clinical practice, the myocardial time-velocity curve can be reconstructed either on line as spectral pulsed TDI or offline from 2D color-coded TDI image loops.[58]

Pulse wave tissue Doppler imaging (PWTDI) can be seen as the precursor of the more recent Doppler myocardial imaging (DMI) modalities. PWTDI allows for recording of a high-quality Doppler profile of the motion of cardiac structures (e.g. mitral ring). It provides a spectral display of the peak tissue velocities.[59] Limitation of pulsed TDI is that simultaneous recording of different ventricular wall segments is not possible. Because TDI in pulsed mode is characterized by high temporal but low spatial resolution, differentiation between subepicardial and subendocardial myocardial velocities is not possible. Most importantly, the single-point velocity method of spectral tissue imaging does not differentiate between actively contracting and passively moving tissue.

In color-coded TDI each pixel of the Doppler spectrum is colored depending on the direction and mean velocity of the motion of the structures within the field of view. Thus, objects moving towards the transducer are colored red, while those moving away from it are colored blue. The advantages of color Doppler mapping include the capacity for rapid visual qualitative assessment of movement of structures, good spatial

resolution allowing differentiation of the velocity profiles between subepicardial and subendocardial layers of myocardium and the ability to analyze simultaneously various myocardial segment. Major disadvantage of color-coded TDI is poor temporal resolution.

As with conventional Doppler echocardiography, TDI requires the beam to be aligned parallel to the direction of movement of the structures of interest for accurate assessment. Therefore, the angle between the ultrasound beam and the direction of movement should not exceed 15°. Another limitation of TDI is related to the fact that the heart performs complex rotational and translational movements inside the chest, thus distorting the measurements of myocardial velocities.

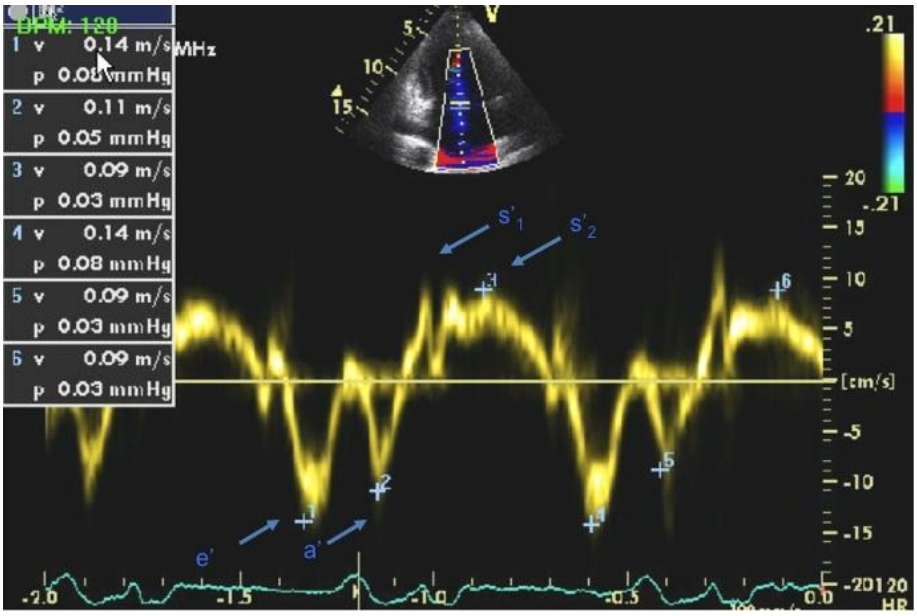

Figure 4. Pulsed Doppler tissue Doppler imaging (TDI) of the mitral annulus. s'$_1$:tissue velocity wave in the isometric contraction period, s'$_2$:velocity wave in the ejection period, e' and a': velocity wave in early and late diastolic periods, respectively.

TDI can be applied to the assessment of both regional and global LV function. Measuring velocities of myocardial segments gives information about regional ventricular contractility, while the measurement of mitral annular velocities provides information on overall longitudinal LV function. Regardless of the site of the measurement, the normal TDI profile has a characteristic appearance. It consists of a systolic (s') wave and early (e') and late (a') diastolic waves. The systolic wave often has two peaks s'$_1$ and s'$_2$. S'$_1$ reflects isovolumic contraction, while s'$_2$ occurs during

ejection (Figure 4).

Myocardial velocities tend to decrease from the mitral annulus to the apex. The magnitude of myocardial velocities also depends on the mode of TDI used. In pulsed mode, velocities (peak) are higher than in color Doppler mode (mean velocities). However, the character of velocity traces does not depend on the mode of scanning.[60]

Currently, TDI is an integral part of an echocardiography examination in various areas of cardiology.

3.1.6 Myocardial strain imaging

Myocardial velocities measured with TDI may be overestimated or underestimated by translational motion or tethering of the myocardium, respectively. This limitation can be overcome by measuring the actual extent of myocardial deformation (stretching or contraction) by strain (ε) and strain rate imaging (SRI).[58] Strain is a representation of myocardial deformation or change in length during systole and diastole. It can be measured utilizing either TDI or, more recently by 2D echocardiographic speckle tracking derived parameters. Strain is a dimensionless index, and reflects the total deformation of the myocardium during cardiac cycle relative to its initial length. For example, if the velocities measured at all points within a moving object are the same, than the object would be described as having displacement. If, on the other hand, different points within an object are moving at different velocities, then the object will exhibit deformation and alter its shape.[54] This is the definition of Langranian strain.

Because myocardial deformation or strain is caused by contraction, strain is a measure of myocardial contractile function.[61] By convention, lengthening is represented as a positive value for strain, while shortening is represented by a negative value.[62] Strain allows for the differentiation of active vs. passive movement within a myocardial segment. Strain rate (SR) is the rate of change (reflects how fast regional myocardial shortening or lengthening occurs) in length calculated as the difference between two velocities normalized to the distance between them; it is expressed as seconds^{-1}. For example, if we assume 20% total Lagrangian strain of a one dimensional object (e.g. the object lengthens from its original length of 2 cm to 2.4 cm) and if the total deformation takes 2 seconds, the average strain rate is equal to 0.20/2 seconds, which is 0.1 s^{-1}: on average, the object lengthens by 10% every second. When the same amount of

deformation occurs in only half this time period (in this example: 1 second) the average strain rate doubles to 0.20/1 second = 0.2 s^{-1}: on average, the object lengthens by 20% every second. [62] The technique of tissue Doppler derived strain and SR is illustrated in Figure 5. A major limitation of this technique is its dependence on the angle of incidence between the ultrasound beam and myocardial motion. Furthermore, high frame rate imaging, ideally > 130 frames per second (FPS), is required for this type of imaging.

Speckle tracking echocardiography (STE) is an alternative and innovative way to obtain myocardial tissue motion information. 2D strain imaging techniques measure Langrangian strain and SR by tracking echocardiographic B-mode speckles (Figure 6), natural acoustic markers, or acoustic backscatter generated by ultrasound interactions (reflection, scattering and interference) within the myocardium (generally made up of 20-40 pixels). The geometric shift of each speckle represents myocardial motion and can be tracked frame to frame, thus allowing for the calculation of strain and SR. See Figure 7. Specialized software for temporal and spatial tracking provides a pattern recognition algorithm to achieve the most accurate derivation for strain. The optimal frame rate for speckle tracking is between 50 and 70 FPS.[58]

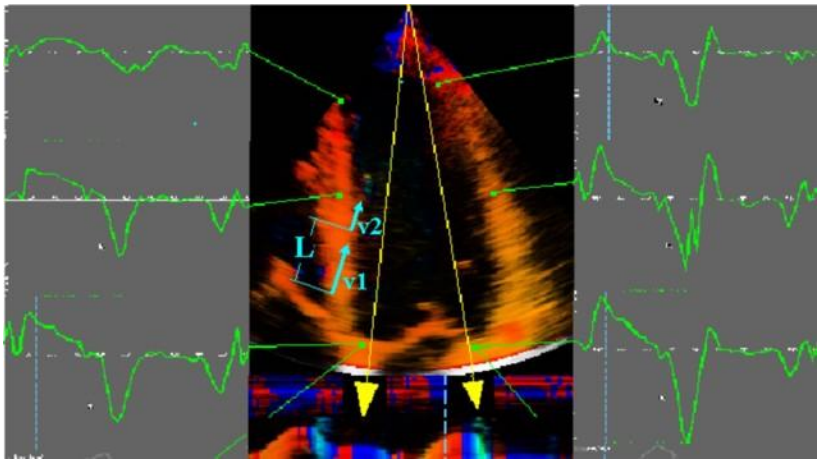

Figure 5. Tissue Doppler derived strain imaging. The difference in velocities (velocity gradient) between two different regions (v_1 and v_2) at a known distance (L) is measured; this allows for the calculation of strain rate (SR): $(v_1-v_2)/ L$; Strain (ε) can be back calculated by using the temporal integration of the SR ($\varepsilon=\int SR \times dt$).

DOI:10.14753/SE.2012.1723

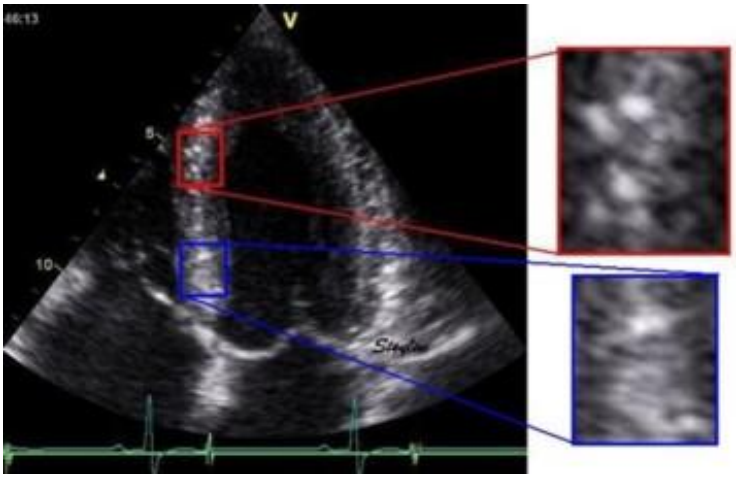

Figure 6. Typical speckle pattern in the myocardium. The two enlarged areas show completely different speckle patterns, which is due to the randomness of the interference. This creates a unique pattern for any selected region, providing both identification of the region and the degree of displacement of the region in the next frame.

Previous studies have depicted LV architecture as a transmural continuum between two helical fiber geometries, where right-handed helical geometry in the subendocardial region gradually changes into lefthanded geometry in the subepicardial region.[63, 64] Thus, cardiac motion is a complex process involving rotation, contraction, and shortening.[65]

STE is simple to perform, it requires only one cardiac cycle, and further processing and interpretation can be done offline. The software only requires harmonic and high frame rate imaging. The real power of speckle analysis is the ability to examine several components or planes (i.e. radial, longitudinal and circumferential) in a single data set.

Myocardial strain quantification by STE has been well validated, using sonomicrometry and tagged cMR as reference methods.[66] STE strain measurements are accurate, with minimal bias and low intra- and interobserver variabilities, and are valid in patients with and without wall motion abnormalities. More recently, STE has been used to evaluate new indices of systolic function, particularly longitudinal strain.[67]

DOI:10.14753/SE.2012.1723

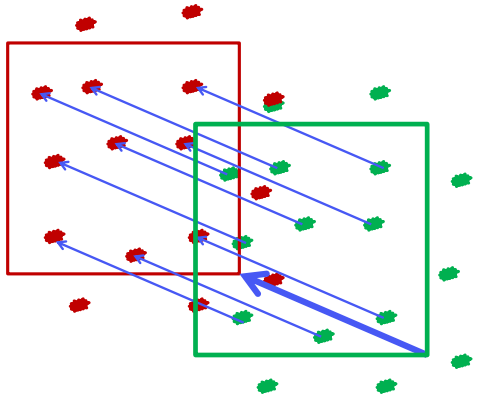

Figure 7. Speckle tracking technique. In the speckle tracking technique, a defined region (Kernel) is tracked, following a search algorithm trying to recognize the most similar speckle pattern from one frame to another. The initial frame is shown in green. Within a defined search area, the new position of the kernel in the next frame (red) can be recognized by finding the same speckle pattern in a new position, indicating that each speckle has moved the same distance in the same direction (thin blue arrows). This allows measurement of the movement of the whole kernel (thick blue arrow), which is the same distance as that of the individual speckles.

STE also offers the unique opportunity to assess torsional deformation of the LV. Indeed, LV contraction not only generates shortening and thickening, but also torsion. Due to the orientation of LV muscle fibres varying across the LV wall – from a right hand helix in the subendocardium, through circumferential fibres in the midwall, to a left hand helix in the subepicardium – the shortening of obliquely oriented LV fibres generates a wringing motion responsible for LV torsion.[68. 69] During the cardiac cycle, a systolic twist and an early diastolic untwist are generated by opposite basal and apical rotations. When viewed from the apex during systole, the apex rotates counter clockwise relative to the base. Torsion, or twist, plays an important role in ejection and in the storage of potential energy at end systole, the release of this energy as elastic recoil during early diastole assists ventricular suction.[67]

For the investigations detailed in this thesis we performed all strain and strain rate measurements by 2D STE.

DOI:10.14753/SE.2012.1723

4 Objectives

The objectives of the present dissertation were the followings:

- to assess the characterization of the mitral and tricuspid annular velocity changes by tissue Doppler imaging in patients with constrictive pericarditis (CP) who underwent pericardiectomy in order to get further insight into the mechanism of annulus motion in CP and to define the diagnostic threshold between primary and secondary CP subgroups,
- to investigate the usefulness of the ratio of medial/lateral strain measurement by speckle tracking echocardiography in the differential diagnosis of CP from restrictive myocardial diseases,
- to perform an analysis of the 189 echocardiography-guided endomyocardial biopsy (EMB) procedures in search of new complications previously undetected by fluoroscopy alone and to describe the characteristics, procedural details, clinical significance and treatment of patients who developed an acute right sided thrombus during the procedure and
- to determine the potential role of speckle myocardial imaging (SMI) for identifying left ventricular dysfunction in patients with isolated left ventricular non-compaction (iLVNC) who have no evidence on two- dimensional imaging or standard Doppler of cardiac impairment and to establish which of the SMI modalities is the most accurate for detection of early left ventricular dysfunction in patients with iLVNC.

DOI:10.14753/SE.2012.1723

5 Methods

The study population consisted of a total of 366 patients in the four presented studies, 288 (99 patients with CP, 189 patients who underwent endomyocardial biopsies), retrospectively enrolled patients between January 2006 and April 2009 and 80 (15 patients with CP, 15 with CA and 20 with iLVNC and 40 control subjects) prospectively enrolled patients between July 2006 through 2009 at the Cardiovascular Division of Mayo Clinic, Rochester, Minnesota. The protocols of the studies were approved by Institutional Review Board of Mayo Clinic. Informed consent was given to patients enrolled in the studies. All patients underwent comprehensive echocardiographic examination.

5.1 Methods and patients in tissue Doppler imaging study of constrictive pericarditis

From January 2006 through September 2008, 183 patients had pericardiectomy at the Mayo Clinic, Rochester, Minnesota. We excluded 41 patients who had pericardiectomy due to recurrent or relapsing pericarditis but no evidence of CP. Also excluded were 43 patients who had concomitant valve surgery or coronary artery bypass grafting at the time of pericardiectomy. Hence, the study population consisted of 99 patients (72 men and 27 women; mean age, 58±15 years) with surgically proven CP who had comprehensive echocardiographic examination before and after pericardiectomy. Since concomitant myocardial disease can affect annulus velocities, we divided patients into 2 groups based on the underlying etiology of CP, i.e. primary CP (idiopathic, postpericarditis, viral etiology; n=52) and secondary CP (due to surgery or radiation; n=47). The clinical profile and echocardiographic findings for both groups were compared before and after pericardiectomy.

Echocardiography examination. All patients had comprehensive evaluation with M-mode, 2-D and pulsed-wave Doppler echocardiography with a respirometer recording and TDI before and after pericardiectomy. Left ventricular ejection fraction (LVEF) was calculated by 2D echocardiography with a modification of the method of Quinones et al.[70] Left atrial volume was measured by the modified biplane area-length method.[71] Right ventricular systolic function was visually assessed. From the mitral inflow

velocities by pulsed wave Doppler echocardiography, the following variables were measured: peak velocities of early (E) and late filling (A) and E wave deceleration time (DT). Peak annular velocities were measured from the apical four chamber view at systole (s'), early (e') and late (a') diastole with a 2–5 mm tissue Doppler sample volume placed at the septal corner and at the mitral and tricuspid lateral annuli. In patients with atrial fibrillation (AF), five consecutive signals were measured and averaged.

Diagnosis of constrictive pericarditis. Clinical, hemodynamic and echocardiographic findings were considered but the final diagnosis of CP was confirmed at the time of surgery in all study patients.

Operative details. Pericardiectomy was performed via a sternotomy or left thoracotomy incision. The standard pericardial resection at our institution is comprehensive, with removal of the diaphragmatic component, the anterior pericardium from phrenic nerve to phrenic nerve as well as that posterior to the left phrenic nerve. In most patients, radical pericardiectomy was performed. Where this was not achievable, as much pericardium was resected as possible. Visceral pericardium was also removed as required.

Statistical analysis. Descriptive data are reported as mean ± SD or count (percent), as appropriate. The Shapiro-Wilk test was used to check the normality of the outcome distributions. Paired t-tests (or Wilcoxon signed-rank tests for non-normal data) were used to assess the echocardiographic parameters before and after pericardiectomy. In addition, comparisons between 2 groups were done with the t-test (or Wilcoxon Rank-Sum test for non-normal data). Differences were considered statistically significant at $p< 0.05$. For all outcomes, Spearman correlations were computed. All analyses were performed using JMP statistical software (version 8, SAS Institute Inc., Cary, NC)

5.2 Methods and patients in speckle tracking imaging study of constrictive pericarditis and restrictive cardiomyopathy

For the differential diagnosis of CP and RCM, a total of 45 patients (15 patients with CP, 15 patients with cardiac amyloidosis (CA) and 15 control subjects) who agreed to join the present study and gave informed consent were prospectively enrolled from patients undergoing evaluation in the Cardiovascular Division at the Mayo Clinic,

Rochester Minnesota, from December 2008 through September 2009 referred for an echocardiogram. Other inclusion criteria were left ventricular ejection fraction (LVEF) > 45%, age > 18 years old and clinically stable patients. Exclusion criteria were more than moderate degree of valvular heart disease, difficult echocardiographic images and present regional wall motion abnormalities. The control subjects were selected from colleagues or trainees who agreed to join the study.

All patients with CP had clinical and echocardiographic evidence of increased right-sided filling pressures. Additional tests for assessment of CP included computed tomography (CT) in 7 patients (47%), CMR in 7 patients (47%), coronary angiography and assessment of cardiac hemodynamics using cardiac catheterization in 8 (53%) patients. Pericardial thickening were noted in 7 patients and calcification were noted in 4 patients by CMR or CT.

RCM was defined as myocardial disease that was characterized by restrictive physiology demonstrated by Doppler transmitral diastolic flow velocity, reduced diastolic LV volumes and LVEF >45%. The underlying etiology of RCM was biopsy proven systemic amyloidosis in all cases.

Echocardiography examination was performed on the patient in the left lateral decubitus position using Artida (Toshiba, Japan) with a PST-30SBT probe. The thickness of the ventricular septum and LV and LV posterior wall, the end-systolic and end-diastolic LV diameters were determined from M-mode or two-dimensional imaging and LV mass and EF were calculated. Left atrial volume measurement and pulsed wave Doppler of mitral inflow were carried out as previously described.[78] Both LV mass and left atrial volume were indexed to body surface area. Peak annular velocities were measured from the apical 4-chamber view at peak annular systole (s'), early (e') and late (a') diastole with a 2-to-5-mm sample volume placed at the septal corner and at the mitral and tricuspid lateral annuli by tissue Doppler echocardiography.

The longitudinal strain was assessed by 2D Speckle Tracking Analysis from apical 4-chamber views using wall motion tracking software (Toshiba, Artida). Following manual initialization of the LV endocardial border, endocardial contours were tracked automatically frame by frame, with the papillary muscles included in the LV cavity. Epicardial contours were manually adjusted when necessary to optimize the boundary position. The LV segments were divided into basal, mid and apical segments. The ratios

of the medial/lateral strains were assessed. Frame rates were set in 50 to 70 Hz in this study.

Statistical analysis. Continuous variables are expressed as mean ± standard deviation. Continuous variables were assessed with the paired t test. Univariate logistic regression was used to predict disease status (constriction vs. restriction) and areas under the curve were calculated. Specific cut points were investigated and specificities and sensitivities were calculated for those cut-points. A value of $p< 0.05$ was considered significant.

5.3 Methods and patients in the echocardiography guided endomyocardial biopsy study

We identified all patients who underwent endomyocardial biopsy at Mayo Clinic, Rochester MN from June 2008 to April 2009 and retrospectively reviewed all the charts of patients undergoing echocardiographic guided endomyocardial biopsies. At Mayo Clinic, echocardiography is used as a supplemental imaging modality to guide EMB in patients undergoing EMB to diagnose myocardial diseases in patients with ventricular dysfunction or who are undergoing surveillance biopsies who are less than 3 month post transplant. Patients who undergo biopsies beyond 3 months post transplant usually have the procedure performed under fluoroscopic guidance alone since cardiac perforation is considered unlikely. We recorded the indication for EMB, route of biopsy, number of biopsy specimens taken and whether the procedure was complicated by thrombus formation.

The EMB undertaken in these patients was performed as follows: in the cardiac catheterization laboratory, either the right internal jugular, or the right or left femoral vein was prepped and draped. After instillation of a local anesthetic agent, the right or left femoral/ right internal jugular vein was entered using the percutaneous technique. An 11cm sheath (ranging in caliber from 7 to 9 French) was placed if an internal jugular vein approach was used. If a trans-femoral route was used an 8 French Mullins sheath was inserted into the femoral vein. Next, a bioptome (ranging in caliber from 6 to 9 French), manufactured by Cordis or Scholten Surgical, was inserted into the sheath and advanced to the right ventricle. Once the position of the bioptome tip was in an ideal location, guided by transthoracic echocardiography (see below), an endomyocardial biopsy was obtained. After each biopsy the bioptome was removed from the heart and

reinserted until a satisfactory number of specimens had been obtained. The venous sheaths were not routinely flushed during the procedure. After the last biopsy specimen had been obtained, the bioptome and sheath were removed and pressure was applied to the puncture site until hemostasis was achieved. The procedure was performed under fluoroscopic and echocardiographic guidance.

Echocardiographic imaging was performed using iE33 Philips transthoracic machine with an S5-1 probe and GE Vivid I laptop machine with a GE 3S-rs probe. Harmonic imaging was routinely used to optimize image quality. The patient was imaged in the cardiac catheterization laboratory while lying supine on the procedure table. Generally, the patient was already prepped and draped prior to imaging. No specific echocardiographic views were obtained. Generally scanning was performed left-handed from the left side of the bed and apical or para-apical views were obtained. Attention was paid to obtain the best longitudinal axis images of the right atrium and right ventricle, tricuspid valve and tricuspid apparatus as well as ensuring the bioptome tip could be visualized in the right ventricle prior to biopsy. Baseline imaging was performed immediately before the procedure and then imaging repeated during bioptome insertion, positioning and biopsy and immediately on withdrawal of the bioptome to evaluate for tricuspid regurgitation and assess for a pericardial effusion. This imaging sequence was repeated for each biopsy attempt until the conclusion of the case. Occasionally, due to poor apical window image quality a subcostal window was used.

5.4 Methods and patients in speckle tracking imaging study of isolated noncompact cardiomyopathy

For the early detection of myocardial impairment in isolated left ventricular non-compaction, the following methods and patient population were used. Exclusion criteria included age < 18 years old, history of moderate or greater systemic or pulmonary hypertension, significant valvular heart disease, clinical or electrocardiographic evidence of ischemic heart disease and evidence of concomitant complex congenital heart disease. Controls (group I) were selected from patients undergoing clinically-indicated echocardiography who had no cardiac symptoms, and no history of hypertension or cardiac disease. They were referred to the echocardiography laboratory

for atypical chest pain (n=6), low-intensity systolic murmur at physical examination (n=4), or to define risk of imminent non-cardiac surgery (n=10). Patients with iLVNC were divided in two groups based on the EF: patients with an EF > 50% (n = 10) were labeled as group II; patients with EF ≤ 50% (n = 10) were labeled as group III.

All ultrasound examinations were performed with a commercially available echocardiographic instrument (Vivid 7; GE Healthcare, Milwaukee, WI). The thickness of the ventricular septum and LV posterior wall, the end-systolic and end-diastolic LV diameters were determined from M-mode or 2D imaging, and LV mass and EF were calculated as previously described.[72] Pulsed wave Doppler of mitral inflow, and LV outflow was performed as previously described.[72] Pulsed wave tissue Doppler Imaging (PWTDI) was measured placing the sample volume on the medial mitral annulus in the apical 4-chamber view. Off-line analysis of standard echocardiographic variables was performed with the use of dedicated software (ProSolv CV analyzer version 3.0); three consecutive beats were measured and averaged for each measurement.

For SMI, apical 4-chamber, long axis, and 2-chamber views were acquired, as well as parasternal short axis view at basal, mid and apical LV level, as previously described (Figure 8).[73] In addition, narrow sector views were acquired for each left ventricular wall from apical views. 2D recordings were collected with a frame rate ranging from 60 (full apical views) to 160 (narrow sector views) frames/sec during brief breath hold. Three consecutive cardiac cycles were recorded as 2D cine loops and the acquired raw data were saved on magneto optical disks or DVDs for offline analysis.

Longitudinal systolic peak values were determined for myocardial velocity (sMV), displacement (sD) strain rate (sSR) and strain (sS). Longitudinal early diastolic peak values were determined for myocardial velocity (dMV-E) and strain rate (dSR-E). Radial and circumferential systolic and early diastolic peak values were measured for sSR, dSR-E, and sS. For longtudinal SMI, analysis was performed considering a model of 18 LV segments individually and also combining them in clusters according to two different criteria. The first criterion was determined by LV level (basal, middle and apical). The SMI values (sMVI, dMV-E, sD, sSR, dSR-E, and sS) were averaged for the 6 basal segments (basal mean), for the 6 middle segments (middle mean) and for the 6 apical segments (apical mean). The second criterion was determined by LV wall. The SMI values were averaged for the anterolateral, inferoseptal, posterior, anteroseptal,

inferior and anterior walls. The averaged LV rotation and rotational velocity profile from six segments of short-axis views at the basal and apical levels were used for the calculation of LV torsion as elsewhere described.[74] After procurements of LV rotation at the two short-axis levels, LV torsion was calculated as the net difference between LV rotation angles obtained from basal (clockwise) and apical (counterclockwise) short axis planes at the same time point, that is, LV torsion (degree) = (apical LV rotation - basal LV rotation).

In the current version of the software used for the measurement of SMI values (Echopac BT09, GE Vingmend Ultrasound Medical Systems, Milwaukee, Wisconsin, USA), the tracking quality for each segment was automatically evaluated and summarized in the tracking table as V (valid tracking) and X (not acceptable tracking).

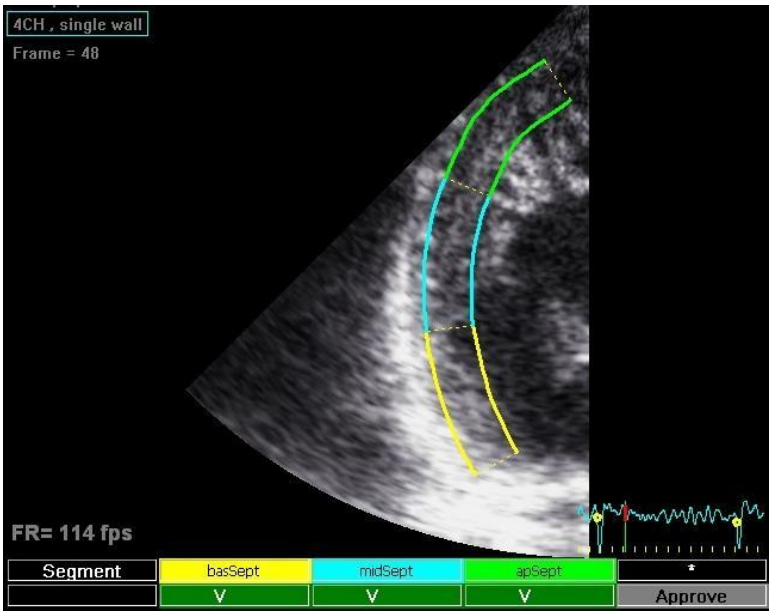

Figure 8. Speckle tracking of the lateral wall (apical 4 chamber, narrow view) in a patient with overt isolated left ventricular non-compaction. The image was analyzed offline with the help of a specific software (ECHOPAC BTW09 GE Vingmend Ultrasound medical systems), tracking quality for each segment is reported at the bottom of the figure.

Cardiac magnetic resonance. ECG-gated CMR was performed on a 1.5T system (Twin speed EXCITE, GE Healthcare, Waukesha, WI, Figure 9) and consisted of steady-state free precession (SSFP) cine-imaging using an eight-element phased-array cardiac coil for signal reception. Left ventricular function was obtained with cine images

using a steady-state free precession (SSFP) technique (TR/TE, 3.5/1.4; matrix, 192 x 192; field of view, 34 x 34 cm; slice thickness, 8 mm) obtained in 2-chamber, 4-chamber, and short-axis planes.

Assessment of the CMR's was performed by one observer by off line measurements of the compacted and non-compacted myocardium in each segment of the 17 segment model.

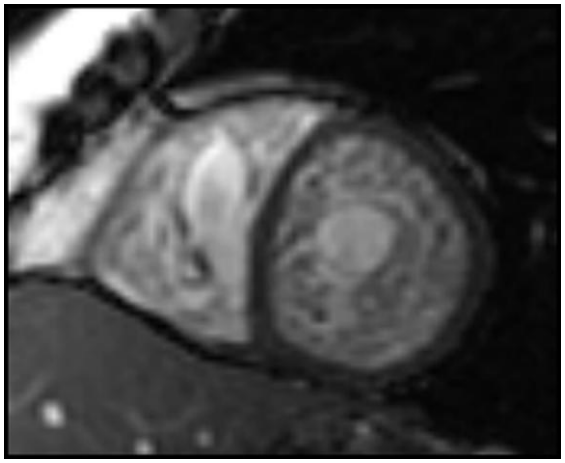

Figure 9. Short axis cardiovascular magnetic resonance (CMR) of a steady state free precession (SSFP) image illustrating severe myocardial trabeculation with deep intertrabecular recesses. Biventricular myocardial involvement with features consistent with non-compaction can be appreciated.

Statistical analyses were performed with a commercially available software program (STATA v10.1, STATA Institute, Cary, TX, USA). Pairwise comparisons between groups were made by Wilcoxon Rank Sum test, Fisher exact test, or exact inference for ordered contingency tables. For measurements of the longitudinal sS at the basal, mid, and apical segments, considering each group separately, a repeated-measures analysis of variance (ANOVA) containing group and segment effects was carried out and the group-segment interaction was fitted. Differences across the three segments within each group were compared using ANOVA for repeated measures. A p-value less than 0.05 for repeated-measures ANOVA was considered statistically significant. Diagnostic accuracy of the SMI modalities (longitudinal, radial, circumferential and rotation/torsion), including global mean values, mean value for clusters and measurements for individual LV segments, was compared by the receiver operating characteristics (ROC) curves for patients with iLVNC and EF > 50% vs controls.

Formal comparisons of the areas under the ROC curves (AUC) were performed as well, using the method of Delong and Delong[75] for comparing AUC between two tests performed on the same subjects.

To examine intra-observer variability (repeatability), a sample of 10 echocardiographic examinations was randomly selected for masked review by the same investigator. To examine inter-observer variability a co-investigator blinded to the clinical information and to the results of the first investigator examined 10 randomly selected echocardiographic exams. Intraclass correlation coefficients (ICCs) for the same observer and different observers were calculated using previously described formulae76 for single segments and for the global mean of each DMI modality. Data are expressed as mean value ± SD, or count (percent). A difference was considered statistically significant when the p-value was less than 0.05.

6 Results

6.1 Results in tissue Doppler imaging study of constrictive pericarditis

To assess the characterization of the mitral and tricuspid annular velocity changes in patients with CP who underwent pericardiectomy, the following results were obtained. Of the 99 patients, CP was secondary to previous cardiac surgery in 34 (34.4%), previous radiation therapy in 13 (13.1%), other causes (postpericarditis, autoimmune, etc.) in 19 (19.2%), and idiopathic in 33 (33.3%). Their mean age was 58±15 years; 72 (73%) were men; patients in the secondary CP group were older (61±13 vs. 53±16 years, p=0.0053). Sinus rhythm was present in 83% of primary CP patients and 83% of secondary CP. Body mass index was 28.5±5 vs. 27.5±5 kg/m^2, and body surface area was 1.99±0.3 vs. 1.98±0.2 m^2, respectively.

Two-dimensional and Doppler echocardiography. Follow-up echocardiograms were obtained 51±131 (range, 0 to 778 days) days after pericardiectomy. Table 1 lists 2D and Doppler echocardiographic data before and after pericardiectomy. Before pericardiectomy, biatrial enlargement was reported in 26 (50%) primary and 32 (68%) secondary CP patients. Apart from mitral A velocity, there were no significant differences between the two subgroups before pericardiectomy. Following

pericardiectomy, only LV end-diastolic dimension was significantly different between these subgroups.

Prior to pericardiectomy, RV function was normal or mildly decreased in 95% of patients, and moderate to severely decreased in 5%. After surgery, these proportions were 81% and 19%, respectively.

DOI:10.14753/SE.2012.1723

	Before pericardiectomy				After pericardiectomy					
	All patients	**Primary CP**	**Secondary CP**	**P∗**	**All patients**	**Primary CP**	**Secondary CP**	**P∗**	**P†**	**P‡**
LVEDD (mm)	43±6	43±6	43±5	0.72	44±6	45±6	42±5	0.045	0.008	0.58
LVESD (mm)	28±4	28±4	28±4	0.25	28 (24,32)	29±5	28±6	0.30	0.11	0.87
LVEF (%)	59±7	60±7	58±7	0.12	60 (54,66)	62 (55,66)	59±10	0.50	0.68	0.26
LAVI (ml/m^2)	33 (28,45)	33 (26,40)	32 (29,52)	0.46	48±17	47±14	48±17	0.71	0.004	0.036
E (m/s)	0.9 (0.7,1.1)	0.9±0.3	0.9 (0.7,1.2)	0.21	1.0 (0.8,1.2)	1±0.2	1.0 (0.8,1.3)	0.36	0.07	0.93
A (m/s)	0.5 (0.4,0.6)	0.5 (0.4,0.6)	0.5 (0.5,0.7)	0.023	0.6 (0.4,0.7)	0.6±0.2	0.6±0.2	0.31	0.039	0.17
E/A	1.7 (1.4,2.2)	1.8 (1.5,2.3)	1.6 (1.3,2.1)	0.42	1.9±0.8	1.9±0.9	1.9±0.7	0.99	0.73	0.76
DT (ms)	155±31	154±31	156±32	0.87	156±33	164±35	148±24	0.06	0.10	0.36

Table 1. General two-dimensional and Doppler echocardiographic parameters in 99 patients with constrictive pericarditis (CP). ∗comparing primary and secondary CP values, †comparing pre- and post-pericardiectomy values in primary CP, ‡comparing pre- and post-pericardiectomy values in secondary CP, not normal distribution values shown as: median (25th, 75th percentile), A: late diastolic velocity of mitral inflow; DT: deceleration time; E: early diastolic velocity of mitral inflow; E/A: early/late filling ratio; LAVI: left atrial volume index; LVEDD: left ventricular end-diastolic diameter; LVEF: left ventricular ejection fraction; LVESD: left ventricular end-systolic diameter, NS: not significant.

Tissue Doppler imaging. Table 2 shows the TDI data points available for analysis, and Table 3 their overall mean values. Among analyzable patients, a medial e' velocity ≥ 8 cm/s was present prior to pericardiectomy in 86% of the entire group, and in 100% of primary and 75% of secondary CP cases.

Between primary and secondary CP groups, there were significant differences in e' velocities except at the tricuspid annulus (Table 4). In both primary and secondary CP groups, early annular diastolic velocities decreased significantly after pericardiectomy (Figure 10, Figure 11, Figure 12, Figure 13, Figure 14, Figure 15), whether medial e' ($p<0.0001$ and $p=0.0004$, respectively), mitral lateral e' ($p=0.022$ and $p=0.013$, respectively) or tricuspid lateral e' ($p=0.0005$ and $p=0.028$, respectively, Table 4). Overall, the reduction in medial e' was somewhat more significant than mitral lateral e' velocity ($p<0.0001$ and $p=0.0004$, respectively, Table 3).

	Prepericardiectomy			**Matched pre- and post-pericardiectomy data**		
	s'	**e'**	**a'**	**s'**	**e'**	**a'**
Medial	92	92	77	76	75	59
Mitral lateral	48	49	41	30	31	24
Tricuspid lateral	39	40	34	18	19	17

Table 2. Frequency of baseline (prepericardiectomy) and matched pre- and post-pericardiectomy tissue velocity data in 99 patients with constrictive pericarditis. The fewer a' values reflect the occurrence of atrial fibrillation. s': systolic annulus velocity, e': early diastolic annulus velocity, a': late diastolic annulus velocity.

DOI:10.14753/SE.2012.1723

	Before pericardiectomy			After pericardiectomy			P value*		
	s'	**e'**	**a'**	**s'**	**e'**	**a'**	**P s'**	**P e'**	**P a'**
Medial	7.0 (6.0,9.0)	12.2	8.0 (7.0,11.5)	6.0 (5.0,7.0)	8.0 (6.0,1.0)	7.0 (5.0,8.0)	<0.0001	<0.0001	<0.0001
Lateral mitral	8.0 (6.3,9.8)	11.9	10.0	6.9	8.0 (7.0,11.0)	7.4	0.017	0.0004	0.016
Lateral tricuspid	12.1	13.1	13.8	6.9	7.5	7.5 (5.0,9.0)	<0.0001	<0.0001	0.0002

Table 3. Overall mean long-axis annular velocities before and after pericardiectomy. All velocity values are in cm/s. *comparing before and after pericardiectomy, s': systolic annulus velocity; e': early diastolic annulus velocity; a': late diastolic annulus velocity. Not normal distribution values shown as: median (25th, 75th percentile).

DOI:10.14753/SE.2012.1723

	Before pericardiectomy				After pericardiectomy				
	All patients (cm/s)	**Primary CP (cm/s)**	**Secondary CP (cm/s)**	**P***	**All patients (cm/s)**	**Primary CP (cm/s)**	**Secondary CP (cm/s)**	**P†**	**P‡**
Medial s'	7.0 (6.0, 9.0)	9.0 (7.0,10.0)	6.0 (5.0,8.0)	0.0002	6.0 (5.0,7.0)	6.4±1.7	6.0 (5.0,7.8)	<0.0001	0.038
Mitral lateral s'	8.0 (6.3,9.8)	9.1±2	7.0 (6.0,9.0)	0.002	7.1±2.2	7.9±1.7	6.5±2.4	0.09	0.11
Tricuspid lateral s'	11.2±3.8	12.4±3.1	9.7±4.0	0.029	7.2±2.7	6.9±2.9	7.6±2.9	0.0005	0.043
Medial e'	12.2±4.2	14.6±3.4	10.3±3.5	<0.0001	8.0 (6.0,1.0)	9±2.9	7.0 (6.0,9.0)	<0.0001	0.0004
Mitral lateral e'	11.6±3.5	12.8±3.8	10.3±2.8	0.008	8.0 (7.0,11.0)	10.0 (8.5,13.0)	7.6±2.0	0.022	0.013
Tricuspid lateral e'	12.2±4.9	13.1±4.8	11.2±4.8	0.20	7.5±2.7	8.4±2.8	6.8±2.4	0.0005	0.028
Medial a'	8.0 (7.0,11.5)	10.0 (7.0,13.0)	8.0 (7.0,10.0)	0.040	7.0 (5.0,8.0)	6.0 (5.0,8.0)	7.2±2.9	<0.0001	0.06
Mitral lateral a'	10.3±4.3	10.5±4.9	10.1±3.5	0.79	8.2±3.4	7.8±3	8.5±3.9	0.08	0.12
Tricuspid lateral a'	11.7±5.4	13.1±5.7	9.6±4.5	0.06	7.5 (5.0,9.0)	8.0 (6.0,9.5)	6.0 (5.0, 9.0)	0.003	0.06

Table 4. Long-axis systolic (s'), early diastolic (e') and late diastolic (a') annular velocities before and after pericardiectomy. All velocity values are in cm/s. *comparing primary and secondary constrictive pericarditis (CP), †comparing pre- and post-pericardiectomy values in primary CP, ‡comparing pre- and post-pericardiectomy values in secondary CP; Not normal distribution values shown as: median (25th, 75th percentile). s': systolic annulus velocity, e': early diastolic annulus velocity, a': late diastolic annulus velocity.

DOI:10.14753/SE.2012.1723

	Before pericardiectomy				After pericardiectomy					
	All patients	**Primary CP**	**Secondary CP**	**P***	**All patients**	**Primary CP**	**Secondary CP**	**P***	**P†**	**P‡**
E/e' medial	7.5 (4.8,10)	6.7±4	8.9 (6.4,14.0)	0.0008	11.2 (7.2,18)	11.7±9	11.2 (8.7,18.4)	0.22	<0.0001	0.22
E/e' lateral mitral	8.3 ±4	7.5±4	9.4±5	0.12	12 (7.3,17)	11±6	13.7 (10,20)	0.022	0.05	0.012
E/e' lateral tricuspid	8.0 (6.0,10.0)	7.1 (5.0, 9.0)	9.2 (6.9,16.5)	0.048	14.3±8	12.5±6.4	16±10	0.10	0.13	0.05
e' lateral mitral /e'medial	0.93 (0.78,1.07)	0.9±0.2	0.94 (0.85,1.2)	0.52	1.1 (0.85,1.5)	1.2 (0.95,1.5)	1.0 (0.8, 1.6)	0.22	0.0006	0.035

Table 5. Early diastolic velocity of mitral inflow (E) to early annular velocity (e') ratios and lateral mitral to medial e' ratio before and after pericardiectomy. *comparing primary and secondary constrictive pericarditis (CP), †comparing pre- and post-pericardiectomy values in primary CP, ‡comparing pre- and post-pericardiectomy values in secondary CP, not normal distribution values shown as: median (25th, 75th percentile).

Comparing radiation and postcardiac surgery patients within the secondary CP group, there were no significant differences in tissue velocity characteristics before or after pericardiectomy. In both groups, medial and mitral lateral e' velocities were lower after surgery. However, the decline in e' appeared more significant in the radiation compared to the cardiac surgery group (p=0.0092 vs. p=0.0383), consistent with greater myocardial disease in the former.

Table 5 shows the E/e' and mitral lateral/medial e' ratios before and after pericardiectomy. Mitral lateral/medial e' velocity ratio was reversed (i.e. less than 1) in 74% of all analyzable cases before pericardiectomy. This reversed ratio prevailed equally in primary (74%) and secondary CP patients (75%), and increased in both CP groups after pericardiectomy (p=0.0002 for the entire CP group). Notably, among primary CP patients, this relationship changed from an overall reversed ratio to normal after surgery (p=0.0006).

There were significant differences in all s' velocities between the subgroups before pericardiectomy. After pericardiectomy, only lateral s' was lower in the secondary group (Table 4). Moderate to strong correlations were observed between s' and e' as well as between s' and a' velocities before pericardiectomy (Table 6). These correlations were in general weaker after pericardiectomy.

	Before pericardiectomy		**After pericardiectomy**	
	s' and e'	**s' and a'**	**s' and e'**	**s' and a'**
Medial (cm/s)	0.62 (<0.0001)	0.66 (<0.0001)	0.34 (0.001)	0.38 (0.001)
Lateral mitral (cm/s)	0.49 (0.0004)	0.41 (0.007)	0.48 (0.0007)	0.44 (0.005)
Lateral tricuspid (cm/s)	0.34 (0.037)	0.81 (<0.0001)	0.27 (0.19)	0.45 (0.034)

Table 6. Spearman correlation of annular velocities before and after pericardiectomy. Data presented as ρ (P value). s': systolic annulus velocity, e': early diastolic annulus velocity, a': late diastolic annulus velocity.

Regional wall motion abnormalities were present in 3 (6%) and 9 (19%) patients with primary and secondary CP, respectively. No significant changes occurred in annular velocities after surgery in these patients, probably due to their small number or lower

baseline annular velocities. Conversely, among the patients without wall motion abnormalities, all annulus velocities decreased significantly ($p<0.03$ for all medial, mitral lateral and tricuspid lateral velocities).

Postoperative echocardiography showed persistent features of CP (defined as at least two of the following: mitral E respiratory variation, hepatic vein diastolic flow reversals with expiration, inferior vena cava plethora) in 7 patients. At the medial annulus where postoperative data were available in all cases, s', e' and a' were not significantly different between these patients and the 92 without persistent constrictive hemodynamics (all $p>0.35$).

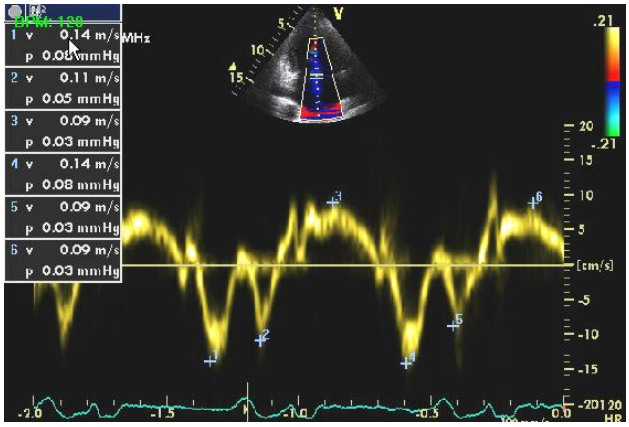

Figure 10. Tissue Doppler Imaging **(**TDI) at the medial annulus in a patient with constrictive pericarditis before pericardiectomy. All subsequent figures are from the same patient. Medial s' 0.09 m/s, e' 0.14 m/s, and a' 0.11 m/s. s': systolic annulus velocity, e': early diastolic annulus velocity, a': late diastolic annulus velocity.

DOI:10.14753/SE.2012.1723

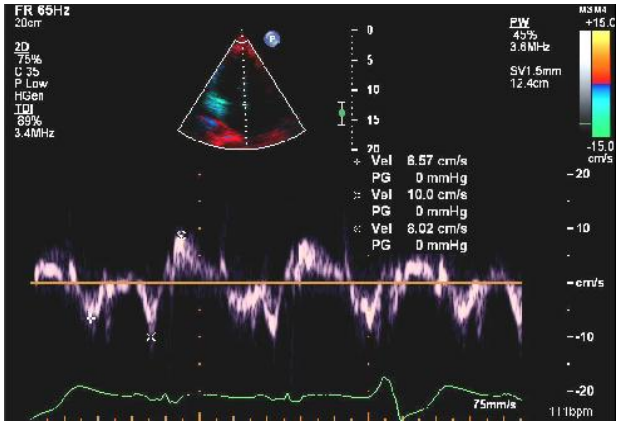

Figure 11. Tissue Doppler Imaging **(**TDI) at the medial annulus after pericardiectomy. Medial s' was 0.08 m/s, e' 0.07 m/s, and a' 0.1 m/s. s': systolic annulus velocity, e': early diastolic annulus velocity, a': late diastolic annulus velocity.

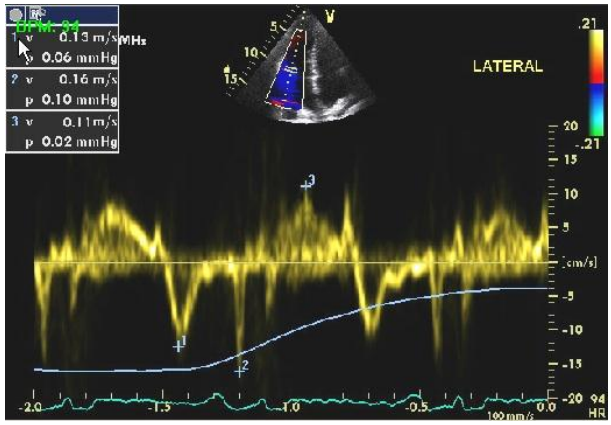

Figure 12. Tissue Doppler Imaging **(**TDI) at the lateral mitral annulus before pericardiectomy. Lateral s' was 0.11 m/s, e' 0.13 m/s, and a' 0.16 m/s. s': systolic annulus velocity, e': early diastolic annulus velocity, a': late diastolic annulus velocity.

DOI:10.14753/SE.2012.1723

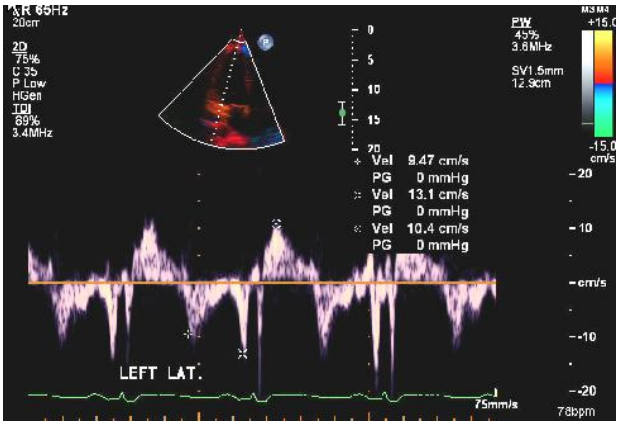

Figure 13. Tissue Doppler Imaging **(**TDI) at the lateral mitral annulus after pericardiectomy. Lateral s' was 0.9 m/s, e' 0.1 m/s, and a' 0.13 m/s. s': systolic annulus velocity, e': early diastolic annulus velocity, a': late diastolic annulus velocity.

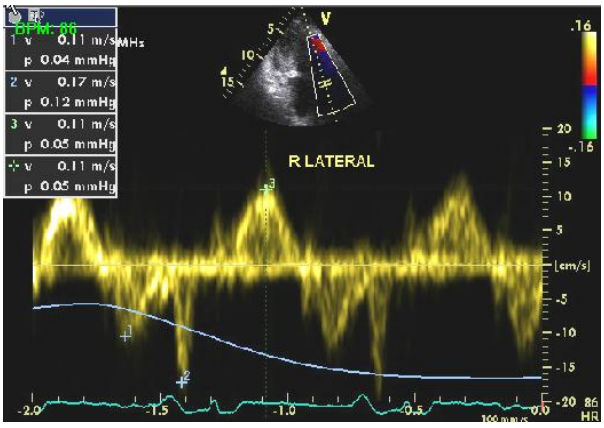

Figure 14. Tissue Doppler Imaging **(**TDI) at the lateral tricuspid annulus before pericardiectomy. Lateral annular s' measures 0.11 m/s, e' 0.11 m/s, and a' 0.17 m/s. s': systolic annulus velocity, e': early diastolic annulus velocity, a': late diastolic annulus velocity.

DOI:10.14753/SE.2012.1723

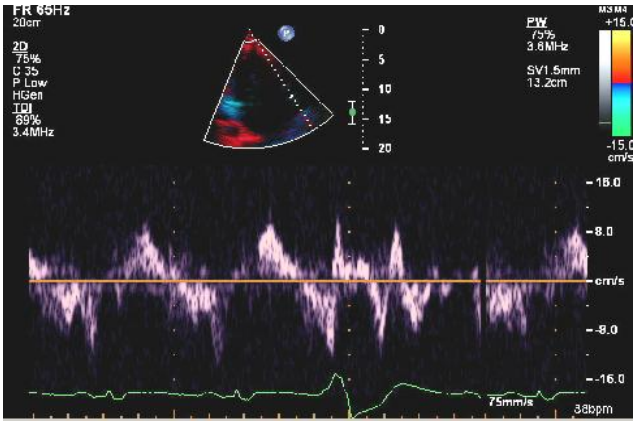

Figure 15. Tissue Doppler Imaging **(**TDI) at the lateral tricuspid annulus after pericardiectomy. Lateral annular s' was 0.09 m/s, e' 0.08 m/s, and a' 0.11 m/s. s': systolic annulus velocity, e': early diastolic annulus velocity, a': late diastolic annulus velocity.

6.2 Results in speckle tracking imaging study of constrictive pericarditis and restrictive cardiomyopathy

For the differential diagnosis of CP from RCM by STE the study patients were classified into 3 groups, CP, CA and control group. There were 19 men in the study, mean age was 52±17 years (56±15 vs. 65±8 vs 34±8) in the three groups, respectively). All patients were in sinus rhythm, two patients from the CP group had paroxysmal atrial fibrillation. The underlying cause of CP was previous cardiac surgery in 1 patient (7%), radiotherapy in 3 patients (20%), idiopathic in 7 patients (46%) and other (autoimmune, viral) in 4 patients (27%). All patients with CP had clinical and echocardiographic evidence of increased right-sided filling pressures. There were no significant differences between CP and CA in cardiac output, 5.6 l /min vs 5.5 l /min in heart rate (HR), 75/min vs 70/min, in (body surface area) BSA 1.97±0.3 (m^2) and 1.9 ±0.3 (m^2). Body mass index (BMI) were 28.9 ±7.6 kg/m^2 and 25.2 ±5.3 kg/m^2, respectively. However, there was a significant difference between CP and CA in LV mass, 100.2 g vs 225.8 g, $p<0.0001$, in LAVI 34.0±13.2 cc/m^2 vs 46.4±10.2 cc/m^2, $p=0.0146$. Pericardial or pleural effusion was present in 8 patients in the CP group. Further echocardiographic parameters are displayed in Table 7 and Table 8. For the longitudinal strain parameters see Table 9. Longitudinal strain was significantly higher for CP in comparison with CA in both the septal and lateral basal segments and in the mid lateral segment, whereas for

mid septal segment there was no such relationship. There were also significant differences in the longitudinal strain basal septal/ basal lateral (BS/BL) and mid-septal and mid-lateral (MS/ML) ratios.

A gradient of longitudinal strain was observed from base to mid segments. The mid longitudinal strain values tended to be higher in both medial and lateral segments, than the base values. Lateral strain values were decreased, where there was calcification or wall thickening. Septal values were preserved.

Parameters	Control Group	Constrictive Pericarditis	Cardiac Amyloidosis	P
LVEF (%)	61±4	65±9	56±10	NS
E (m/sec)	0.75±0.1	0.9±0.2	0.8±0.3	NS
A (m/sec)	0.5±0.09	0.6±0.3	0.5±0.3	NS
E/A	1.5±0.3	1.9±0.9	2.4±2.3	NS
Septum (mm)	8.6±1.8	9.2±2.2	15.5±3	<0.0001
PW (mm)	8.5±1.6	9.9±1.2	14.9±3.5	<0.0001
LVEDD (mm)	48±4	45±5	43±8	NS
LVESD (mm)	34±7	29±5	30±7	NS

Table 7. Standard echocardiographic parameters in patients with constrictive pericarditis, cardiac amyloidosis and control group. LVEF: left ventricular ejection fraction; E: early diastolic filling of mitral inflow; A: late diastolic filling of mitral inflow; PW: posterior wall; LVEDD: left ventricle end-diastolic diameter; LVESD: left ventricle end-systolic diameter; P: comparing constrictive pericarditis and cardiac amyloid group. NS: non-significant. Values are presented as mean ± standard deviation.

DOI:10.14753/SE.2012.1723

Parameters	Normal	Constrictive Pericarditis	Cardiac Amyloidosis	P
Medial s'	0.133±0.2	0.08±0.02	0.044±0.009	<0.0001
Medial e'	0.125±0.02	0.122±0.03	0.038±0.13	<0.0001
Medial a'	0.092±0.02	0.094±0.03	0.054±0.03	0.004
Lateral mitral s'	0.086±0.02	0.080±0.02	0.048±0.01	<0.0001
Lateral mitral e'	0.15±0.03	0.106±0.02	0.046±0.02	<0.0001
Lateral mitral a'	0.083±0.01	0.091±0.04	0.051±0.02	0.018
Lateral tricuspid s'	0.123±0.02	0.102±0.03	0.11±0.03	NS
Lateral tricuspid e'	0.14±0.03	0.1±0.02	0.09±0.03	NS
Lateral tricuspid a'	0.103±0.02	0.114±0.04	0.106±0.005	NS

Table 8. Mitral and tricuspid annular velocities (m/s) in constrictive pericarditis, cardiac amyloidosis and control group. s': systolic annulus velocity; e'; early diastolic annulus velocity; a': late diastolic annulus velocity, P: comparing constrictive pericarditis and cardiac amyloid group. Values are presented as mean ± standard deviation.

Parameters	Control group	Constrictive Pericarditis	Cardiac Amyloidosis	P
Longitudinal strain BS (%)	-13.6±2.29	-15.5±3.4	-5.25±3.74	<0.0001*
Longitudinal strain BL (%)	-17.04±1.85	-12.9±5.1	-8.45±4.13	0.0231*
Longitudinal strain MS (%)	-19.56±2.15	-17.6±4.9	-10.35±5.4	0.0002*
Longitudinal strain ML (%)	-21.00±2.77	-13.31±4.96	-13.49±6.52	NS
Longitudinal strain BS/BL	0.8±0.11	1.3±0.51	0.6±0.31	00002*
Longitudinal strain MS/ML	0.94±0.12	1.5±0.91	0.85±0.56	0.0302*

Table 9. Longitudinal peak systolic strain values and ratios obtained by speckle tracking echocardiography in constrictive pericarditis, cardiac amyloidosis and control group. BS: basal septum; BL: basal lateral; MS: mid septum; ML: mid lateral; P:

comparing constrictive pericarditis and cardiac amyloid group. NS: non-significant. Values are presented as mean ± standard deviation.

Statistical analysis. There is a statistically significant association between the BS/BL longitudinal strain ratio and the disease status (constriction vs. restriction), p=0.02. Using a cut point of the BS/BL longitudinal strain ratio of 1.02, there was a sensitivity of 0.91 (91%) and a specificity of 0.93 (93%) of detecting CP. Sensitivity and specificity of BS/BL potential cut points are displayed in Table 10. See Figure 16 for ROC for BS/BL. For MS/ML in general, specificities and sensitivities were fairly good (at cut point of 0.96, sensitivity was 0.93 (93%) and specificity of 0.87 (87%) for detecting CP) however, there was no statistically significant association between the MS/ML longitudinal strain ratio and the disease status (constriction vs. restriction), p=0.08 (Table 11, Figure 17).

Cut points:	**>1.34**	**>1.12**	**>1.02**	**>0.74**
Sensitivity (%)	45	45	91	100
Specificity (%)	100	93	93	67

Table 10. Sensitivity and specificity of longitudinal strain ratios of basal lateral and basal septal left ventricular segments at potential cut points.

Cut points	**>1.00**	**>0.96**	**>0.95**	**>0.94**
Sensitivity (%)	93	93	100	100
Specificity (%)	100	87	87	80

Table 11. Sensitivity and specificity of longitudinal strain ratios of mid lateral and mid septal left ventricular segments at potential cut points.

DOI:10.14753/SE.2012.1723

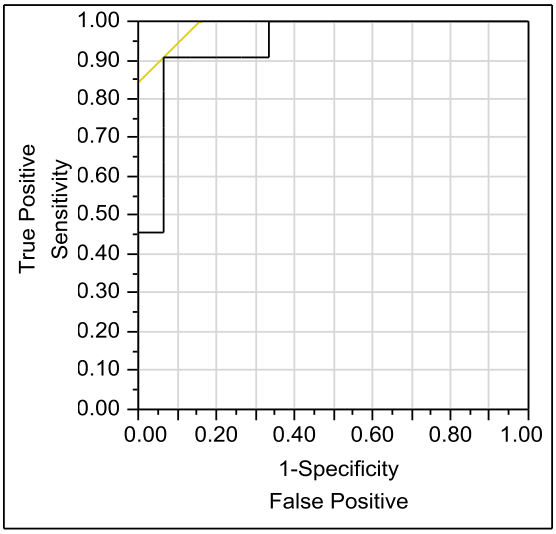

Figure 16. Receiver operating characteristics (ROC) curve for basal septal to basal lateral (BS/BL) left ventricular segment ratios; Using 1=constrictive pericarditis (CP), 2=cardiac amyloidosis (CA)='1' to be the positive level; Area Under Curve = 0.93939.

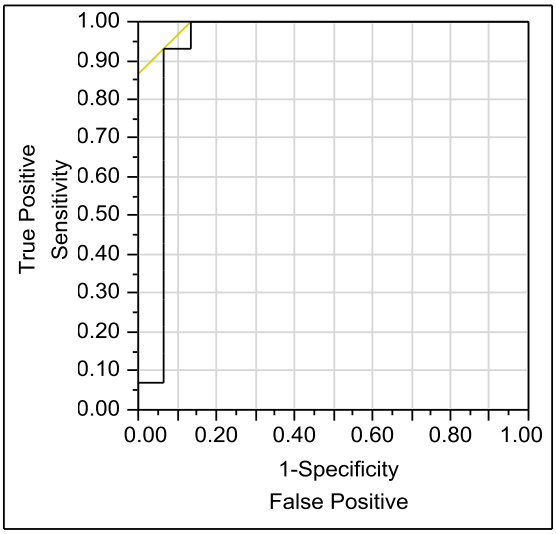

Figure 17. Receiver operating characteristics (ROC) curve for mid-septal to mid-lateral (MS/ML) left ventricular segment ratios; Using 0=norm,1=constrictive pericarditis (CP), 2=cardiac amyloidosis (CA) ='1' to be the positive level; Area Under Curve = 0.93333.

DOI:10.14753/SE.2012.1723

6.3 Results in the echocardiography guided endomyocardial biopsy study

There were 415 RV biopsies performed in 212 patients at Mayo Clinic from June 2008 to April 2009. Of these biopsy procedures, 189 were echocardiography guided (undertaken in 90 patients). 135 of these biopsies (71.4%) were performed for transplant surveillance, 40 biopsies (21.1%) for evaluation of etiology of left ventricular dysfunction and 14 biopsies (7.4%) to rule out cardiac amyloid. The route of EMB was most frequently from the right internal jugular vein (77.3%). Access via the right femoral vein was used in 21.1% of cases and the left femoral vein in 1.6%. Most commonly, 5 biopsy specimens were obtained per procedure (76.2%) with a range of 0 to 8 biopsy specimens.

In 8/189 (4%) of the echocardiography guided procedures acute thrombus was identified at the time of the biopsy, usually towards the end of the procedure, in seven patients (1 patient experienced acute thrombus formation on two separate occasion) (Figure 18). Although the majority of procedures were performed from a right internal jugular approach acute thrombus formation occurred in only 3/143 (2%) of these procedures. Thrombus occurred most frequently when a right femoral vein access site was used; 5/35 procedures (12.5%). The left femoral vein was used in only 3 procedures and no thrombus developed in any of these cases. There was no clear association between number of biopsy specimens obtained and risk of thrombus. Of the eight procedures in which thrombi were detected, 5 biopsies were performed in 3 procedures, 3 biopsies in 2 procedures, and 1, 6 and 7 biopsies in 1 procedure each.

DOI:10.14753/SE.2012.1723

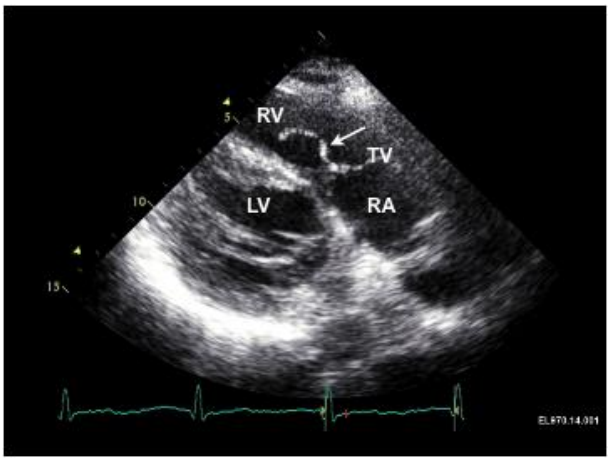

Figure 18. Modified parasternal right ventricular inflow view in Patient 2 demonstrating a 5 cm highly mobile serpiginous thrombus attached to the tricuspid valve (TV) that developed at the time of endomyocardial biopsy. RA: right atrium, RV: right ventricle, LV: left ventricle.

Clinical and echocardiographic characteristics of patients who developed thrombi. The mean age of the 7 patients who developed thrombi during endomyocardial biopsy was 48 ± 10 years. 3 were male. The indication for the biopsy was surveillance of heart transplantation in 6 patients (representing 5.2% of echocardiographic guided transplant surveillance EMB procedures) and evaluation for suspected cardiac amyloid in 1 patient (7.1% of echocardiographic guided EMB procedures to detect cardiac amyloid). Histology ultimately confirmed a diagnosis of cardiac amyloid in this patient. Four patients had a history of prior thrombosis and 1 patient had a defined clotting diathesis. Table 12 summarizes the general characteristics and pertinent medical history of all 7 patients in whom thrombi were identified, while Table 13 summarizes the clinical features of the heart transplantation patients in particular. The echocardiographic characteristics of these patients are summarized in Table 14.

Patients	Gender	Age	EMB Indication	Prior Thrombosis	Comorbidities
1	Male	52	HTX	left internal jugular DVT	HL, HT, ICD pre HTX
2	Female	50	HTX	Left cephalic vein thrombosis and right internal jugular DVT	Radiation and chemotherapy for breast cancer, ICD pre HTX
3	Female	48	HTX	right and left subclavian vein DVT, left internal jugular vein DVT, pulmonary embolism	Asthma, steroid induced DM
4	Male	46	HTX	VAD cannula thrombosis, right internal jugular vein thrombosis, TIA	HT, HL, CRT-D pre HTX
5	Male	62	HTX	No	Multiple sclerosis, HT, paralyzed left hemidiaphragm, LVAD infection pre HTX
6	Female	50	Amyloid	Stroke	PPM, colitis, hepatitis B
7	Female	29	HTX	No	Rheumatoid arthritis, thrombocytopenia

Table 12. Clinical characteristics of patients with endomyocardial biopsy (EMB) related thrombosis. HTX: heart transplantation, HL: hyperlipidemia, HT: hypertension, ICD: implantable cardioverter-defibrillator, DVT: deep vein thrombosis, DM: diabetes mellitus, TIA: transient ischemic attack, CRT-D: cardiac resynchronization therapy with ICD, PPM: permanent pacemaker, LVAD: left ventricular assist device.

Regarding the procedural details, three cases were performed via a transjugular approach using an 11cm sheath ranging in caliber from 7 to 9 French inserted into the right internal jugular vein, and 4 via a femoral approach using an 8 French Mullins sheath inserted into the right femoral vein. A bioptome ranging in caliber from 6 to 9 French, manufactured by Cordis (n =4) or Scholten Surgical (n=3), was used in these

cases. See Table 15 for the characteristics of the endomyocardial biopsy in each patient. In one patient (patient #4) unique thrombus formation occurred on two successive EMB attempts, 2 weeks apart. In this patient interval echocardiography confirmed resolution of the index thrombus after treatment with systemic anticoagulation. However, another thrombus formed during subsequent EMB despite continuous flushing and frequent aspiration of the Mullins sheath throughout the procedure.

Pt	HTX Indication	LVAD pre HTX	Complications post HTX	Immunosuppressive medications at time of EMB	Time interval between HTX and EMB
1	Ischemic cardiomyopathy	No	Graft dysfunction, bronchial bleeding, RV dysfunction	cyclosporine, MM, prednisone	7 Weeks
2	Restrictive cardiomyopathy secondary to Adriamycin and radiation	Yes	No	cyclosporine, MM, prednisone	6 Months
3	Eosinophilic myocarditis	Yes	Pulmonary bleeding, loculated pleural effusion, bilateral upper DVT	cyclosporine, MM, prednisone	3 weeks
4	Idiopathic dilated cardiomyopathy	Yes	No	cyclosporine, MM, prednisone	3 Months
5	Ischemic cardiomyopathy	Yes	Colonic perforation	cyclosporine, MM, prednisone	6 Months
7	Idiopathic pulmonary hypertension	No	pleural and mediastinal bleeding, pneumonia and respiratory failure	cyclosporine, MM, prednisone	3 Months

Table 13. Clinical characteristics of cardiac transplant patients with endomyocardial (EMB) related thrombosis. HTX: heart transplantation, LVAD: ventricular assist device, RV: right ventricle, DVT: deep vein thrombosis, MM: mycophenolate mofetil.

Management included either immediate thrombus aspiration or systemic anticoagulation post procedure. There were no overt occurrences of pulmonary thromboembolism. Table 16 summarizes the specific thrombus location and individual patient management in all 8 cases.

DOI:10.14753/SE.2012.1723

Pt	RV size	RVF	TV morphology	TR velocity pre biopsy (m/sec)	TR severity	LV size (diastolic/systolic dimension in mm)	LV EF (%)
1	Mod ↑	Mild ↓	Intact	2.8	mod	45/32	60
2	N	N	Intact	2.5	mild	45/30	66
3	N	N	Intact	3.1	mild	43/24	72
4	N	N	flail segment	2.8	severe	41/28	58
5	N	N	Intact	unable to detect	trivial	48/39	37
6	N	N	Intact	3.1	severe	56/37	65
7	Mild ↑	N	Intact	2.4	trivial	47/33	60

Table 14. Echocardiographic parameters at the time of endomyocardial biopsy (EMB). ↑: increase, ↓: decrease, N: normal, TV: tricuspid valve, LV: left ventricle, EF: ejection fraction, RVF: right ventricular function. Pt: patient

Pt	EMB approach	Sheath French size	Bioptom French size	Heparin post sheath insertion	Cor angio pre EMB	Sample number	Histology
1	Right femoral	8	7	Yes	Yes	5	No rejection
2	Right femoral	8	7	No	No	3	No rejection
3	Right femoral	8	8	No	No	3	Acute rejection
4 *	Right femoral	8	6	No	Yes	7	Acute rejection
4 #	Right femoral	8	7	Yes	No	6	Acute rejection
5	Right IJ	9	9	No	No	1	No rejection
6	Right IJ	7	7	No	No	7	Amyloid
7	Right IJ	9	9	No	No	5	Acute rejection

Table 15. Endomyocardial biopsy (EMB): procedural details. * First occurrence of thrombus in patient 4; # second occurrence of thrombus in patient 4, Pt: patient, IJ: internal jugular.

DOI:10.14753/SE.2012.1723

Pt	Thrombus Location	Thrombus Size (cm)	Management
1	Tip of sheath in RA	2.5	Aspiration
2	RA and RV across TV, emanating from sheath tip	5.0	unsuccessful extraction; IV heparin and warfarin
3	Tip of bioptome in RV	2.0	Extraction
4*	Tip of bioptome in RV	4.6	LMWH
4#	RV apex	1.5	Warfarin
5	RV	0.5	iv heparin
6	Attached to PM lead in RA	2.0	iv heparin, LMWH
7	Tip of sheath in RA	1.3	LMWH

Table 16. Endomyocardial biopsy: thrombus location and management. * First occurrence of thrombus in patient 4; # second occurrence of thrombus in patient 4, RA: right atrium, RV: right ventricle, TV: tricuspid valve, PM: pacemaker, LMWH; low molecular weight heparin, iv: intravenous.

6.4 Results in speckle tracking imaging study of isolated noncompact cardiomyopathy

In the non-compaction patients versus control group the following results were obtained. **Demographic standard echocardiography and CMR data.** Twenty patients comprised the control group (group I), 10 patients had iLVNC with EF >50% (group II) and 10 patients had iLVNC with EF ≤ 50% (group III), with mean EF of 64±4, 58±4 and 34±14 percent, respectively ($p<0.001$ between group III compared to I and II, Table 17). Age and gender distribution were not different between patients and controls (Table 17). Among patients, there were two familial iLVNC pairs (father-son and brother-sister, total four patients) evaluated, all of whom had a family history of sudden cardiac death. Two iLVNC patients had a family history of dilated cardiomyopathy. Among patients with EF ≤ 50% (group III), three subjects were in functional class III/IV whereas no patients in groups I and II were symptomatic. All patients with decreased EF were receiving appropriate medical treatment including ACE-inhibitors and Beta-

blockers. Six patients received prophylactic AICD (Automated Internal Cardioverter Defibrillator) implantation (four in group III and two in group II) with no reported therapeutic shocks. One patient from group III died of complications related to primary pulmonary fibrosis. Although LV wall thickness was not different among groups, LV mass index, LV end-systolic and end-diastolic diameters were all increased in group III compared to group II and controls and not different between group II and controls (Table 17). Although E wave velocity was reduced in group III compared to the other groups, all other measures of trans-mitral flow (A wave and E/A) were not different among the groups. PWTDI e' and s' velocities were lower and E/e' were higher in group III patients compared to the other groups, and not different between groups II and controls (Table 17).

Cardiac magnetic resonance. Presence of hypertrabeculation was assessed for each of 17 LV segments, and involved some middle LV segments and all apical segments, with basal segments spared. For the 15 patients referred for CMR, the ratio of compacted over non compacted segments was not different between groups II and III. Anterior and lateral walls were the most involved (considering all patients together, these walls had 17 and 23 non-compacted segments, respectively).

Longitudinal SMI. Data on longitudinal systolic and diastolic SMI measures are reported in Table 18 and Table 19, respectively. Longitudinal sMV measures were abnormally reduced in group III patients compared to the other groups, and the clusters of LV segments by wall or by level, as well as the global mean of all 18 segments, were not different between group II and group I. Longitudinal sD measures, as well as sSR and sS values, including most of the clusters of segments and the global mean of 18 LV segments, were reduced in group III compared to both groups; they were also significantly reduced in group II compared to group I.

DOI:10.14753/SE.2012.1723

Variable (mean ± SD)	Controls Group I	Non-Compaction EF > 50% Group II	Non-Compaction EF ≤ 50% Group III
Age (years)	41 ± 15	35 ± 13	49 ± 13
Males (%)	13 (65)	7 (70)	4 (40)
NYHA III/IV (%)	0 (0)	0 (0)	3 (30) ‡ ╬
Heart Rate (bpm)	70 ± 13	63 ± 9	63 ± 11
Atrial Fibrillation (%)	0 (0)	0 (0)	1 (10)
PM/ICD (%)	0 (0)	2 (20)	5 (50) ‡ ╬
Ratio of non-compacted to compacted	N/A	2.39 ± 0.6	2.40 ± 0.5
Left ventricular thickness (mm)	10 ± 1.2	10 ± 1.3	10 ± 1.5
Left ventricular mass index (g/m2)	82 ± 17	108 ± 55	156 ± 48 ‡ †
LVEDD (mm)	47.1 ± 4.9	46.1 ± 3.6	57.4 ± 8.9 ₣ ¥
LVESD (mm)	28.3 ± 5.2	30.1 ± 3.6	45.1 ± 12.1 ‡ ¥
E wave velocity (m/s)	0.8 ± 0.2	0.8 ± 0.3	0.6 ± 0.2 ₣
E wave deceleration time (ms)	193.5 ± 36.2	189.1 ± 36.2	209 ± 44.5
A wave velocity (m/s)	0.6 ± 0.1	0.5 ± 0.1	0.6 ± 0.4
E/A	1.5 ± 0.4	1.8 ± 0.4	1.3 ± 0.6
Ejection Fraction (%)	64 ± 4.3	58 ± 4.4	34 ± 13.7 ‡ ╬
Stroke Volume (ml)	93.1 ± 25.9	84.5 ± 7.6	78.2 ± 17.4
Cardiac Index (l/m2/min)	3.4 ± 0.7	2.8 ± 0.3	2.6 ± 0.5 ₣
Medial s' velocity (m/s)	0.08 ± 0.01	0.09 ± 0.04	0.07 ± 0.04
Medial e’ velocity (m/s)	0.08 ± 0.02	0.10 ± 0.03	0.06 ± 0.03 ₣ †
Medial a' velocity (m/s)	0.08 ± 0.01	0.07 ± 0.03	0.07 ± 0.02 §
E/e’	8.4 ± 2.2	9.1 ± 4.7	13.8 ± 7.5 §

Table 17. Clinical, ECG, standard echocardiographic and CMR variables for patients (group II and group III) and controls (group I). Comparisons are made using the pairwise Wilcoxon Rank Sum test, or Fisher exact test. PM/ICD = Pacemaker/IntraCardiac Defibrillator. LVEDD = left ventricle end diastolic diameter; LVESD = left ventricle end systolic diameter, E: early diastolic velocity of mitral inflow, A: late diastolic velocity of mitral inflow, s’: systolic annulus velocity, e’:early

diastolic annulus velocity, a': late diastolic annulus velocity. § = p < 0.05 vs Controls; ₣ = p < 0.01 vs Controls; ‡ = p < 0.001 vs controls; † = p < 0.05 vs Non-Compact. EF > 50%; ¥ = p < 0.01 vs Non-Compact. EF > 50%; ╬ = p < 0.001 vs Non-Compact. EF > 50%.

Variable (mean ± SD)	Controls Group I	Non-Compaction, EF>50% Group II	Non-Compaction, EF≤ 50% Group III
Tissue Velocity Imaging (cm/sec)			
Basal Mean	6.8 ± 1.1	6.2 ± 0.9	4.8 ± 1.6 ₣ †
Middle Mean	5.0 ± 1.1	4.6 ± 0.9	3.8 ± 1.3 §
Apex Mean	3.1 ± 0.9	2.8 ± 0.4	2.6 ± 0.8
Lateral	5.5 ± 1.8	4.9 ± 1.4	4.0 ± 1.6 §
Inferoseptum	4.6 ± 1	4.3 ± 0.9	3.4 ± 1.2 ₣
Posterior	6.2 ± 1.2	5.5 ± 0.8	3.9 ± 1.7 ₣ †
Anteroseptum	3.7 ± 1.2	3.6 ± 1.2	3.2 ± 0.9
Inferior	5.2 ± 1.3	4.8 ± 0.6	3.8 ± 1.6 §
Anterior	4.5 ± 1.4	4.2 ± 1.1	4.0 ± 1.7
Global Average	5.0 ± 0.9	4.5 ± 0.6	3.7 ± 1.2 ₣ †
Displacement (mm)			
Basal Mean	15.7 ± 1.4	13 ± 2.1 ‡	9.5 ± 3.6 ‡ †
Middle Mean	10.7 ± 1.1	8.6 ± 1.5 ‡	6.5 ± 2.3 ‡ †
Apex Mean	5.3 ± 1.0	4.3 ± 1.0 §	3.4 ± 1.2 ‡
Lateral	11.0 ± 3.0	8.0 ± 1.9 §	6.0 ± 1.4 ‡ †
Inferoseptum	10.6 ± 2.2	10.0 ± 3.1	7.2 ± 2.9 ‡ †
Posterior	11.6 ± 1.9	9.8 ± 1.3 ₣	6.1 ± 3.3 ‡ †
Anteroseptum	9.2 ± 2.4	7.4 ± 2.2	5.9 ± 2.3 ₣
Inferior	11.3 ± 2.1	9.4 ± 1.8 ₣	7.1 ± 3.8 ‡
Anterior	9.6 ± 1.8	7.2 ± 2.2 ‡	5.9 ± 2.7 ₣
Global Average	10.6 ± 1.0	8.6 ± 1.4 ‡	6.5 ± 2.3 ‡ †

To be continued on next page

DOI:10.14753/SE.2012.1723

Variable (mean ± SD)	Controls Group I	Non-Compaction, EF>50% Group II	Non-Compaction, EF≤ 50% Group III
Strain Rate Imaging (1/s)			
Basal Mean	-1.4 ± 0.2	-1.3 ± 0.2	-1.0 ± 0.3 ‡ †
Middle Mean	-1.3 ± 0.1	-1.1 ± 0.2 §	-0.9 ± 0.3 ‡
Apex Mean	-1.4 ± 0.2	-1.1 ± 0.2 ‡	-1.0 ± 0.3 ‡
Lateral	-1.3 ± 0.2	-1.2 ± 0.3	-1.0 ± 0.4 §
Inferoseptum	-1.2 ± 0.2	-1.0 ± 0.2 ‡	-0.9 ± 0.2 ‡
Posterior	-1.4 ± 0.2	-1.2 ± 0.3 §	-1.0 ± 0.2 ‡
Anteroseptum	-1.3 ± 0.3	-1.2 ± 0.3	-1.0 ± 0.4 Ŧ
Inferior	-1.4 ± 0.2	-1.2 ± 0.3	-1.0 ± 0.4 ‡
Anterior	-1.4 ± 0.3	-1.2 ± 0.3 §	-1.0 ± 0.2 ‡
Global Average	-1.3 ± 0.2	-1.2 ± 0.2 §	-1.0 ± 0.3 ‡
Strain Imaging (%)			
Basal Mean	-21.4 ± 1.8	-18.0 ± 3.4 Ŧ	-14.1 ± 4.7 ‡ †
Middle Mean	-21.8 ± 1.7	-17.4 ± 3.6 ‡	-13.7 ± 4.9 ‡ †
Apex Mean	-22.6 ± 2.2	-17.0 ± 3.7 ‡	-13.6 ± 4.1 ‡ †
Lateral	-21.1 ± 2.5	-16.0 ± 5.0 Ŧ	-15 ± 5.5.0 ‡
Inferoseptum	-22 ± 2.3	-17.5 ± 2.9 ‡	-12.7 ± 4.0 ‡ Ɏ
Posterior	-21.8 ± 2.2	-17.8 ± 5.2 §	-14.7 ± 4.9 ‡
Anteroseptum	-21.4 ± 3	-18.3 ± 2.7 §	-13.5 ± 7.0 ‡ †
Inferior	-22.8 ± 3.4	-18.8 ± 5.6 §	-14.1 ± 5.8 ‡
Anterior	-21.9 ± 2.8	-16.2 ± 3.4 ‡	-12.6 ± 3.6 ‡
Global Average	-21.9 ± 1.7	-17.4 ± 3.3 ‡	-13.8 ± 4.5 ‡ †

Table 18. Longitudinal systolic SMI modalities and measures for patients (group II and group III) and controls (group I). Single segment measures have been summarized in clusters by level and by wall, and the global mean of 18 LV segments is reported as well. Comparisons are made using the pairwise Wilcoxon Rank Sum test. § = $p < 0.05$ vs Controls; Ŧ = $p < 0.01$ vs Controls; ‡ = $p < 0.001$ vs controls; † = $p < 0.05$ vs Non-Compact. EF > 50%; Ɏ = $p < 0.01$ vs Non-Compact. EF > 50%; ╬ = $p < 0.001$ vs Non-Compact. EF > 50%.

Variable (mean ± SD)	Controls Group I	Non-Compaction, EF>50% Group II	Non-Compaction, EF≤ 50% Group III
Tissue Velocity (cm/sec)			
Basal Mean E	-9.0 ± 1.9	-7.5 ± 2.1	-4.6 ± 2.2 ‡ †
Middle Mean E	-6.9 ± 2.3	-5.2 ± 1.7 §	-3.5 ± 1.2 ‡ †
Apex Mean E	-4.4 ± 1.5	-3.3 ± 1.0 §	-2.5 ± 0.9 ‡ †
Lateral E	-7.3 ± 2.1	-5.5 ± 2.4	-3.9 ± 1.8 ‡
Inferoseptum E	-6.2 ± 1.9	-5 ± 1.6	-3.4 ± 1.3 ‡
Posterior E	-8.6 ± 2.5	-6.7 ± 2.4	-3.7 ± 1.7 ‡ ¥
Anteroseptum E	-5.8 ± 1.7	-4.2 ± 1.2 §	-3.1 ± 1.0 ‡ †
Inferior E	-6.7 ± 2.0	-5.9 ± 1.7	-3.4 ± 1.7 ‡ †
Anterior E	-6.3 ± 2.2	-4.6 ± 1.6 §	-3.6 ± 1.7 ‡
Global Average E	-6.8 ± 1.8	-5.3 ± 1.5	-3.5 ± 1.4 ‡ †
Strain Rate (cm/sec)			
Basal Mean E	2.0 ± 0.4	1.9 ± 0.5	1.3 ± 0.5 ‡ †
Middle Mean E	1.7 ± 0.3	1.4 ± 0.4	1.0 ± 0.4 ‡ †
Apex Mean E	1.9 ± 0.4	1.6 ± 0.4 §	1.1 ± 0.4 ‡ †
Lateral E	1.9 ± 0.5	1.6 ± 0.4	1.5 ± 0.5 §
Inferoseptum E	1.8 ± 0.4	1.7 ± 0.3	1.0 ± 0.4 ‡ †
Posterior E	1.8 ± 0.3	1.7 ± 0.6	1.4 ± 0.5 §
Anteroseptum E	1.8 ± 0.4	1.6 ± 0.3	1.0 ± 0.6 ‡ †
Inferior E	1.9 ± 0.4	1.8 ± 0.8	1.0 ± 0.5 ‡ †
Anterior E	2.0 ± 0.5	1.5 ± 0.6 §	1.0 ± 0.4 ‡
Global Average E	1.9 ± 0.3	1.6 ± 0.4	1.1 ± 0.4 ‡ †

Table 19. Longitudinal diastolic SMI modalities (dMV-E and dSR-E) and measures for patients (group II and group III) and controls (group I). Single segment measures have been summarized in clusters by level and by wall, and the global mean of 18 LV segments is reported as well. Comparisons are made using the pairwise Wilcoxon Rank Sum test. § = $p < 0.05$ vs Controls; ¥ = $p < 0.01$ vs Controls; ‡ = $p < 0.001$ vs controls;

† = p < 0.05 vs Non-Compact. EF > 50%; ¥ = p < 0.01 vs Non-Compact. EF > 50%; ╬ = p < 0.001 vs Non-Compact. EF > 50%.

Repeated measures ANOVA (Figure 19) inspecting longitudinal sS of the basal, mid, and apical LV segments to depict differences across LV level in the same group or a group-level interaction, showed significant differences in group I ($p < 0.0009$) of sS across the basal, middle, and apical segments, being the apical sS, on average, more negative than basal or middle sS. The analysis showed no differences in sS across LV levels in either group II ($p = 0.40$) or group III ($p = 0.63$), although the trend was inverted in patients compared to controls, being the middle and apical sS measures less negative than basal sS. Finally, the group-level interaction was significant ($p < 0.0001$), showing that being in a specific group (I, II, or III), significantly influenced longitudinal sS values at each LV level.

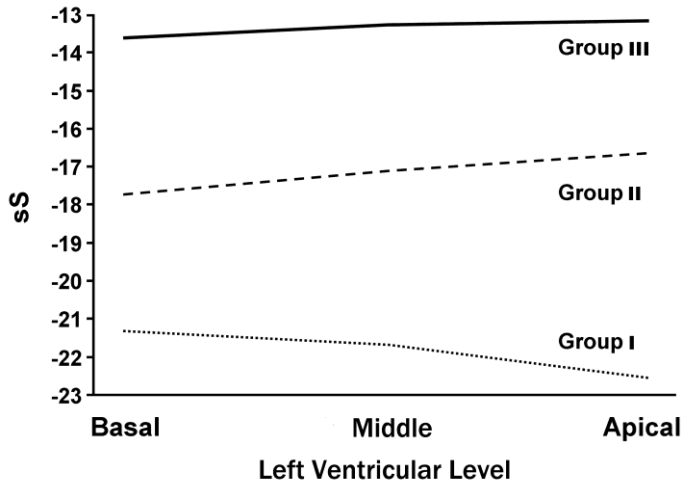

Figure 19. Comparison of longitudinal systolic strain (sS) of the left ventricle at the basal, mid, and apical level, for each group. P values were calculated using repeated-measures analysis of variance and denote differences across 3 segments from the base, mid, and apex, and differences as a result of the interaction of group and level. *: P < .001 comparing the base, mid, and apex within the same group.

Longitudinal dMVI-E and dSR-E values at all LV levels and most LV walls, as well as the global mean of 18 LV segments, were reduced in group III compared to either group II or group I. dMVI-E measures were also significantly reduced in group II compared to

group I considering the mean of the six middle segments, mean of the six apical segments, and the anterior and anteroseptal walls. When compared to group I, patients in group II had a significant reduction of dSR-E values of the mean of the six apical segments and of the LV anterior wall.

Radial and cirumferential SMI, LV rotation/torsion. Radial and circumferential sSR, dSR-E and sS were all reduced in group III compared to the other groups, whereas only radial sS was significantly reduced in group II compared to group I (Table 20).

Variable (mean ± SD)	Controls Group I	Non-Compaction, EF>50% Group II	Non-Compaction, EF ≤50% Group III
Radial sSR (1/s)	2.0 ± 0.6	1.7 ± 0.4	1.2 ± 0.4 ‡ †
Radial dSR-E (1/s)	-2.4 ± 0.7	-2.1 ± 1	-1.4 ± 0.9 §
Radial sS (%)	51.9 ± 12.8	32.7 ± 9.3 ₣	19 ± 12.1 ‡ †
Circ sSR (1/s)	-1.5 ± 0.4	-1.4 ± 0.2	-0.9 ± 0.3 ₣ †
Circ dSR-E (1/s)	1.9 ± 0.4	1.8 ± 0.3	1.2 ± 0.3 ₣ ¥
Circ sS (%)	-20.9 ± 2.8	-18.5 ± 3.2	-12 ± 5.6 ₣ †
Rotation Basal mean (degrees)	-7.6 ± 3.4	-6.0 ± 1.7	-3.9 ± 2.5 §
Rotation Apical mean (degrees)	22.2 ± 12.8	5.0 ± 4.5 ‡	2.3 ± 3.3 ‡
Torsion (degrees)	28.3 ± 12.3	9.6 ± 6.4 ‡	3.9 ± 4.5 ‡ †
Torsion Rate (degrees/s)	171.7 ± 49.8	71.2 ± 29.4 ‡	67.7 ± 43.3 ‡
Untorsion Rate IVRT (degrees/s)	181.4 ± 56.1	101.7 ± 48.7 ₣	59.5 ± 66 ₣ †
Untorsion Rate late (degrees/s)	99.4 ± 62.5	42.6 ± 21.7 ₣	36.9 ± 11.9 ₣

Table 20. Radial, circumferential SMI modalities and LV rotation/torsion measures for patients (group II and group III) and controls (group I). Comparisons are made using the Wilcoxon Rank Sum test. EF: ejection fraction; § = $p < 0.05$ vs Controls; ₣ = $p < 0.01$ vs Controls; ‡ = $p < 0.001$ vs controls; † = $p < 0.05$ vs Non-Compact. EF > 50%; ¥ = $p < 0.01$ vs Non-Compact. EF > 50%; ╬ = $p < 0.001$ vs Non-Compact. EF > 50%.

The LV rotation of the six basal segments was reduced in group III compared to the other groups, whereas it was not different between group II and group I. LV rotation of the six apical segments as well as LV torsion rate and LV untorsion rate at late diastole, were reduced in both group III and group II compared to group I but were not significantly different between group III and group II. LV torsion and the LV untorsion rate at early diastole were reduced in group III compared to either group II or group I and in group II compared to group I as well (Table 20).

ROC analysis. ROC analysis demonstrated that SMI measurement for any single LV segment is not sufficient to accurately discriminate between group II and the controls. Calculation of longitudinal systolic SMI, and specifically the mean of the segments in a level, as opposed to the mean of segments in walls, tended to be the clustering technique providing better discrimination (Figure 20, Figure 21, Figure 22). Considering the global and level means of longitudinal, radial and circumferential sMV, dMV-E, sD, sSR, dSR-E and sS, as well as LV rotation/torsion measures, the longitudinal sS global mean (cut-off value = -19.0 %, sensitivity = 90%, specificity = 100%), sS mean of the six apical segments (cut-off value = -20.0 %, sensitivity = 90%, specificity = 90%), the LV rotation of the six apical segments (cut-off value = 8.0 degrees, sensitivity = 100%, specificity = 90%), LV torsion (cut-off value = 22.0 degrees, sensitivity = 87%, specificity = 89%), and LV torsion rate (cut-off = 110.0 degrees/sec, sensitivity = 93%, specificity = 89%), were the most accurate (greatest AUC) for discrimination between iLVNC patients with EF > 50% (group II) and healthy subjects (group I) and their diagnostic accuracies were not significantly different (p=0.77). Longitudinal sD global mean (cut-off value = 10.0 mm, sensitivity = 75%, specificity = 80%) had high accuracy as well.

Figure 20, Figure 21 and Figure 22 show the ROC analysis for the SMI modalities, the comparison between iLVNC patients and EF > 50% (group II) vs controls (group I) with the following abbreviations: sS global mean = mean of the sS values for 18 LV segments; sS apical mean = mean of the sS values for 6 LV apical segments; sSR apical mean = mean of the sSR values for 6 LV apical segments; sD global mean = mean of the sD values for 18 LV segments; sD middle mean: mean of the sD values for 6 LV middle segments; Radial sS mean = Radial sS mean of the 6 LV segments at level of the papillary muscles in short axis (SAX) view; Circumferential sS mean: circumferential

sS mean of the 6 LV segments at level of the papillary muscles in SAX view; Rotation apical mean: mean of the LV rotation for the 6 LV apical segments; Torsion: LV torsion (computed as (apical LV rotation - basal LV rotation)); Torsion rate: LV torsion rate (degree/s).

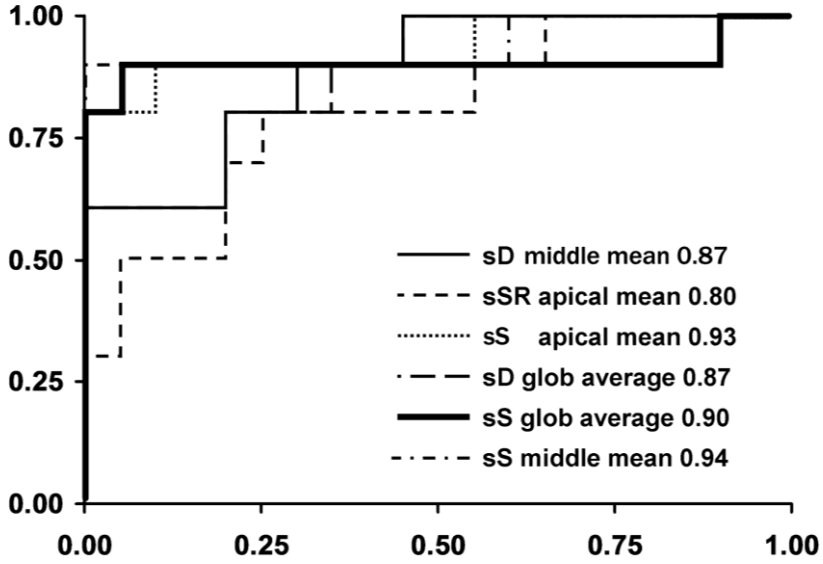

Figure 20. SMI longitudinal measures; AUC's group II vs group I: sS global mean=0.94 (95% CI 0.82 – 1.00); sS apical mean = 0.93 (95% CI 0.82 – 1.00); sS middle mean = 0.90 (95% CI 0.72 – 1.00); sSR apical mean = 0.80 (95% CI 0.63 – 0.98); sD global mean = 0.87 (95% CI 0.74 – 1.00); sD middle mean = 0.87 (95% CI 0.74 – 1.00).

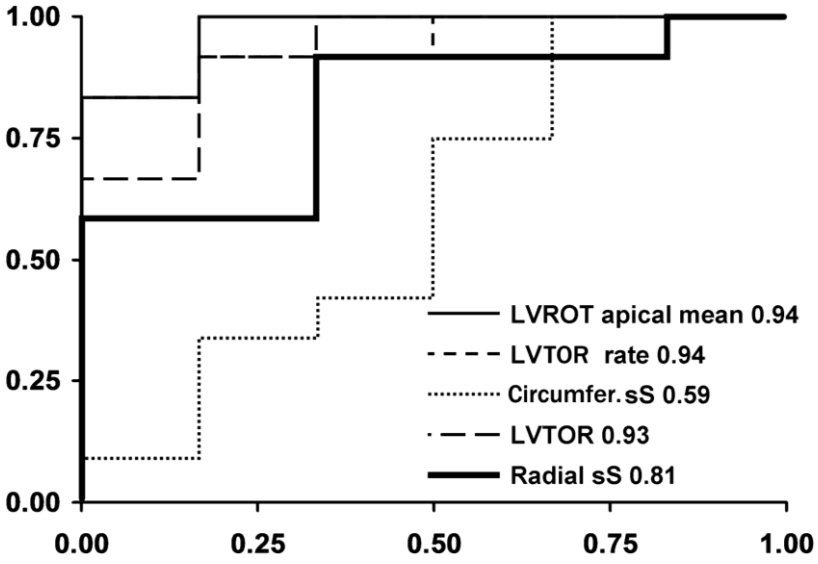

DOI:10.14753/SE.2012.1723

Figure 21. SMI Radial, circumferential, and LV rotation/torsion measures;
AUC's group II vs group I: Radial sS mean=0.82 (95% CI 0.61 – 1.00); Circumferential sS mean = 0.60 (0.26 – 0.93); LV rotation apical mean = 0.94 (95% CI 0.83 – 1.00); LV torsion = 0.93 (95% CI 0.81 – 1.00); LV torsion rate (95% CI 0.84 – 1.00).

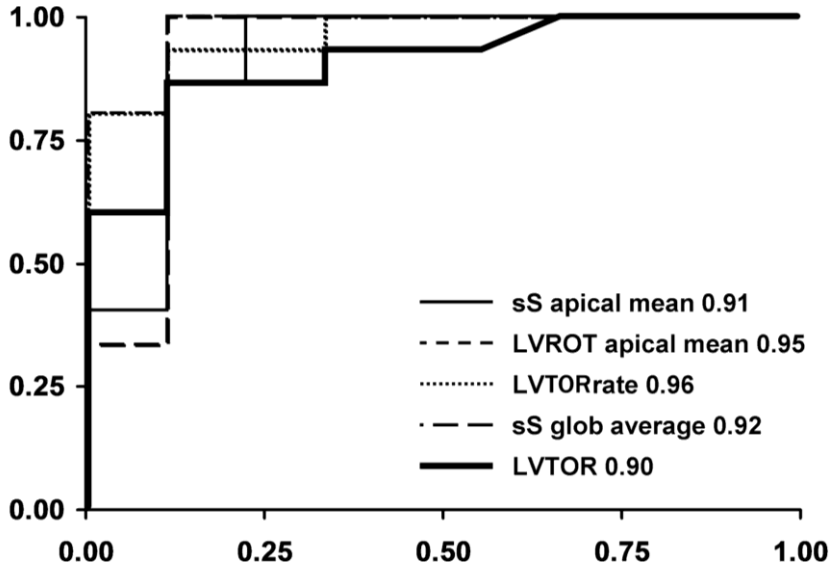

Figure 22. SMI best modalities. AUC's group II vs group I: sS apical mean, sS global mean, LV rotation apical mean, LV torsion, LV torsion rate. P-value for the ROC curves comparison = 0.57.

Intra- and inter-reader reproducibility. The ICC for intra-reader reproducibility was computed for the global sMV (ICC = 0.97), global sD average (ICC = 0.95), global sSR average (ICC=0.93), global sS average (ICC=0.98), radial sS (ICC=0.92), circumferential sS (0.89), LV torsion (ICC=0.91) and LV torsion rate (ICC=0.90).
The ICC for inter-reader reproducibility was computed for the global sMV (ICC=0.95), global sD average (ICC=0.87), global sSR average (ICC =0.88), global sS average (ICC=0.94), radial sS (ICC=0.90), circumferential sS (0.85), LV torsion (ICC=0.86) and LV torsion rate (ICC=0.88).

DOI:10.14753/SE.2012.1723

7 Discussion

Garcia et al. were the first to report that the measurement of longitudinal axis expansion by TDI provided a clinically useful distinction between CP and restrictive RCM. [77] Subsequently, Rajagopalan et al showed that a peak e' velocity ≥ 8 cm/s could discriminate between these entities with high sensitivity and specificity.[23] We have confirmed that medial e' velocity is relatively normal or even accentuated in patients with CP, irrespective of the presence or absence of characteristic respiratory variation in mitral E velocity.[26] Other investigators[24, 25] have recommended the routine measurement of e' in the evaluation of heart failure and/or suspected CP, albeit with interpretive caution in the setting of myocardial disease, patchy fibrosis or extensive annular calcification.[27, 28, 29] Our group first described a reversal of the normal relationship of mitral lateral e' and medial e' velocities in CP i.e. "annulus reversus" whereby mitral lateral e' velocity is lower than medial e' velocity and lateral/medial e' ratio inverted.[35] Few data exist on postoperative changes in TDI – in one study of 16 patients, Kim et al found that medial e' decreased significantly after pericardiectomy.[36] Building on these observations from a small number of patients, our aim was to provide a comprehensive evaluation of TDI at both mitral and tricuspid annuli in a larger number of patients and follow their evolution after pericardial resection.

Early diastolic annulus velocity. We confirmed the presence of "annulus reversus" in patients with CP. Based on the hypothesis that lateral annulus motion is restricted by the constricting pericardium and that medial annulus diastolic motion increases in compensation, it may be anticipated that medial mitral annulus velocity decreases and lateral annulus velocity increases after pericardiectomy, and that mitral lateral/medial e' ratio normalizes. While the latter was confirmed, both medial and mitral lateral e' velocities were found to decrease after pericardiectomy. Several mechanisms may explain these observations. Pericardiectomy removes constraint to lateral expansion of the annuli and nullifies the exaggerated longitudinal motion of the mitral annulus as well as the translational component of lateral e' velocity related to increased medial excursion. In some patients, low annular velocities unmasked by pericardiectomy may reflect underlying myocardial damage or atrophy secondary to long-standing encasement and penetration of the myocardium by calcium spurs[78], persistent

inflammation and since the pericardium might be firmly adherent to the myocardium, additional injury at the time of surgery.

We also found reduced tricuspid lateral e' velocity after pericardiectomy. The aforementioned mechanisms operative at the mitral annuli apply but we note also the relevant and frequent association of CP with significant tricuspid regurgitation, and in some cases further RV expansion and worsening of regurgitation following pericardiectomy.[79]

Diagnostic threshold. The primary and the secondary groups had a mean medial e' of 14.6±3.4 and 9.3±3.4 cm/sec, respectively ($p<0.001$). The optimal cut-off point is 11 cm/sec, with a sensitivity of 88% and specificity of 70%. Although, these values do not provide an absolute differentiation between the primary and secondary groups, they can still provide helpful information in regards to the myocardial involvement when assessing the disease in its complexity. A cut-off point for medial e' value of 8 cm/sec was described by Ha for differentiating CP from RCM with a sensitivity of 95% and a specificity of 96%, suggesting a robust clinical differentiative measure. At this cut-off point, however, our data suggest only 76% sensitivity level within the CP group itself. When applying the cut-off point of 8 cm/sec to our primary and secondary group, it results 100% sensitivity and 37% specificity. This shows that the 8 cm/sec cut-off point would work very well for CP had it only contain the primary group when compared to the same restrictive group as in Ha's analysis. The major difference lays at the nature of the secondary group. Based on patient etiology, secondary/primary group ratio was 78/52. For the subgroups within the secondary group, the medial e' means are lower for the radiation compared to the surgery group (8.7±4 vs 9.4±3.4 cm/sec, NS) and the concomitant secondary surgery group compared to without any concomitant surgery group (7.5±2.3 vs 10.2±3.6 cm/sec, $p=0.0003$). For the number of patients in each group, the respective ratio is 32/46 for the radiation over surgery group and 31/47 for the concomitant over without any concomitant surgery group. All above factors contributed to the 37% specificity of the secondary group below the 8 cm/ sec level during the primary-secondary comparison, when sensitivity for the primary group alone was 100%. This led to a substantially lower overall sensitivity for the entire CP group (76%) when the 8 cm /sec cut-off point was applied. The sensitivity in our analysis for the overall CP group is substantially lower than the one described in Ha's paper. In his

study there were a few prominent differences, such as the smaller number of CP patients (23), relatively less patients with secondary etiology as the secondary/primary ratio was lower (8/15), and within the secondary group only surgery group with typically higher values was present with the total absence of radiation and concomitant surgery patients typically with lower values, as shown in our study. Above factors contributed to the higher CP sensitivity in Ha's analysis for the 8 cm/sec cut-off, which led to its suggestion for the differentiation between CP and RCM. However, our findings on a larger patient pool and more diverse secondary subgroup resulting a 76% sensitivity for the CP group did not confirm the above findings and implies that the medial e' values being lower than 8 cm/sec does not rule out the possibility of CP.

Systolic annulus velocity. S' by TDI reflects the peak velocity of myocardial fiber shortening in the longitudinal direction and provides a more sensitive assessment of global LV systolic function than 2D or M-mode imaging.[80] S' has been correlated with peak positive dP/dt and LVEF in patients with dilated cardiomyopathy, hypertensive heart disease and myocardial infarction.[81, 82, 83] There is little information on mitral and tricuspid s' velocities in patients with CP. Studies in very small patient populations have either compared s' velocity between CP and RCM[84, 85] or changes in s' pre- and post-pericardiectomy.[36, 85]

The mean s' velocity in patients with secondary CP was lower both before and after pericardiectomy than published normative values[34] and also lower, especially pre-pericardiectomy, than those with primary CP. These observations concord with coexisting myocardial disease in this subgroup. In both CP subgroups, all s' velocities decreased after pericardiectomy, consistent with previous smaller studies.[36, 84] This finding seems counterintuitive since s' velocity is expected to increase with augmented stroke volume after pericardiectomy. To explain this paradoxical relationship between s' and stroke volume in CP, we postulate that systolic and diastolic motion of the mitral annulus are closely coupled, in part via elastic recoil mechanisms.[85] Thus, in the pre-pericardiectomy setting, both longitudinal systolic and diastolic motion of the annuli are exaggerated while following release of pericardial constraint, both decrease in tandem. This hypothesis is supported by the moderate to high correlation between annular s' and e' as well as s' and a', especially before pericardiectomy when restorative forces may be most operative.

There appeared to be proportionately greater postoperative reduction in tricuspid lateral or RV s' and e' compared to mitral annulus values. As the pericardial process is often asymmetric, being most pronounced over the RV[86], annular motion here may be expected to be most exaggerated before pericardiectomy, and following decortication, approximate normality. However, the disproportionate reduction in tricuspid lateral s' and e' probably stems also from postoperative RV dysfunction, which was moderate to severe in 1 in 5 patients.

LVEF did not change despite the expected increase in stroke volume after pericardiectomy. We postulate that after pericardial resection, LV filling increases and other elements of LV shortening including torsion are recruitable, contributing to better cardiac output and compensating for abnormal longitudinal function. Sengupta et al[87] found higher net twist but no significant increase in torsion post-pericardiectomy, a conclusion limited by small patient numbers and early timing of the postoperative studies when restoration of function may have been incomplete. To confirm our hypothesis, detailed analysis of myocardial mechanics in a larger number of patients pre- and post-pericardiectomy will be required.

A subset of patients with CP continue to experience heart failure symptoms after pericardiectomy, one cause being residual constriction. In this study, we did not find any significant difference in annulus velocities between patients with and without postoperative constrictive hemodynamics. The utility of TDI in identifying residual CP should be further assessed in larger cohorts with clinical outcomes correlation.

Limitations. Our study was retrospective and has the inherent limitations of this design. Notwithstanding, these observations on TDI in CP represent, to our knowledge, the largest dataset published to date. We only recorded TDI of longitudinal axis motion in the 4-chamber view. Due to the local tethering effect, analysis of multiple annular regions could have provided additional helpful data. It would also be useful to characterize radial and circumferential function for a better understanding of the mechanics of the unique annulus motion in CP and the effects of pericardiectomy. As not all patients had mitral lateral and tricuspid lateral TDI recordings, certain conclusions were drawn from subsets with comparable data. Although this limits power, we do not envisage specific biases in the selective analysis.

The comparison of TDI in patients with primary and secondary CP is confounded by the older age of the latter. Age influences both systolic and diastolic myocardial velocities arising from differences in myocyte integrity, fibrosis and beta-adrenergic receptor density. However, normal TDI reference values[34] indicate that within the one-decade difference in age between patients with primary and secondary CP, a percentage difference between 0% (for medial e') and 13% (for lateral e') can be expected. This contrasts with the observed 19% to 30% difference in TDI values between these groups prepericardiectomy, and from 6% to 32% post-pericardiectomy, suggesting a relatively minor influence of age compared to CP etiology.

In CP there is impaired diastolic filling due to constricting pericardium, whereas in RCM there is myocardial abnormality, which results in abnormal diastolic function. Both disease processes limit diastolic filling and result in diastolic heart failure. The clinical diagnosis of CP and its differential diagnosis from RCM still can be very challenging. Similar symptoms (dyspnea, tachycardia, jugular venous distention, peripheral oedema, etc.) and hemodynamic changes can be seen in both diseases: elevation and equalization of intracardiac diastolic pressures and a prominent dip and plateau in ventricular diastolic waveforms.[8]

Pericardial thickness and calcification are generally increased in CP, however they are difficult to measure by echocardiography, as the quantification of thickening degree by echocardiography is problematic. Moreover 15-20% of patients have been found to have pericardial constriction with normal pericardial thickness by CMR.[2] Besides M-mode and 2D echocardiography, the respiratory variability in transmitral flow velocity is the most frequently used parameter to differentiate CP from RCM.[12] In CP left heart filling is decreasing during inspiration and right heart filling is decreasing during expiration. TDI can be used to quantify longitudinal mitral annular motion, which can be useful in distinction between CP and RCM.[22] However, a considerable percentage of CP patients do not demonstrate respiratory variation[26], and is also found in other diseases, especially in COPD.[14] Furthermore TDI still has some pitfalls especially under certain circumferences, such as annulus calcification and/or ventricular dysfunction.[29, 29, 30] Therefore, the diagnosis of CP remains a diagnostic challenge with important therapeutic implications of surgical cure. Because CP can be caused by different new

etiologies as therapeutic irradiation, cardiopericardial surgery, viral, idiopathic, autoimmune, etc, the differential diagnosis from RCM is even more difficult because it can manifest heterogenously.

In patients with CP, mechanoelastic properties of the myocardium are relatively preserved in the longitudinal direction, and therefore longitudinal deformation of the LV base and longitudinal early diastolic velocities are either normal or exaggerated. Conversely, patients with RCM and intrinsic myocardial abnormalities have reduced longitudinal deformation of the LV base and reduced early diastolic longitudinal velocities.[1] Mitral septal annular velocity is usually increased in patients with CP and higher than the lateral annular velocity.[35] Up to date there were only a few studies, which investigated the longitudinal mechanics in CP and RCM with speckle tracking strain analysis[87], which is an angle-independent technique showing close correlations with measurements obtained by magnetic resonance imaging[88, 89] and sonomicrometry.[90, 91] Sengupta found that patients with CP have relatively preserved longitudinal LV mechanics, markedly abnormal circumferential deformation, torsion and untwisting velocity. In contrast, patients with RCM had abnormal longitudinal mechanics as reduced longitudinal strain, particularly at the LV base with relative sparing of LV rotation.[87] Furthermore, a comparison of the LV mechanics with pericardial thickness, as measured by CT, in patients with CP has shown a significant correlation between decreased circumferential strain and degree of pericardial thickening at the apex.[92]

In our study, we hypothesized that the longitudinal strain of the lateral wall that is in contact with diseased pericardium is lower than that of the medial segments in CP.

Our results confirm Sengupta's finding that patients with CP have relatively preserved longitudinal LV mechanics compared with patients with RCM and that longitudinal shortening strains recorded from the LV basal segments were significantly higher in CP group in comparison with RCM. There was also a significant longitudinal strain difference between the two patient groups recorded in the mid-septal segment. Sengupta averaged 2D strain parameters from 6 segments in short-axis views and from lateral and septal wall segments in apical 4-chamber views, which provided a measure of global LV function. In our study, we analyzed regional longitudinal strains from apical 4-chamber views in the basal and mid-segments of the septum and lateral walls of the left

ventricle and assessed their ratios.

The main findings of the current investigation were as follows: the longitudinal strain of the lateral wall was lower than that of the septal wall in CP (Figure 23), while the reverse was true in the control and CA group (Figure 24 and Figure 25). Therefore, the medial/lateral ratio of longitudinal strain in CP group was higher than that in normal group or cardiac amyloid group. The differential longitudinal strain assessment by STE can be valuable in differentiating CP from restrictive diseases. With a cut point of 1.02, the BS / BL longitudinal strain ratio with a sensitivity rate of 91% and specificity rate of 93%, it can be an additional useful method at the verification of CP and in the differential diagnosis with CA.

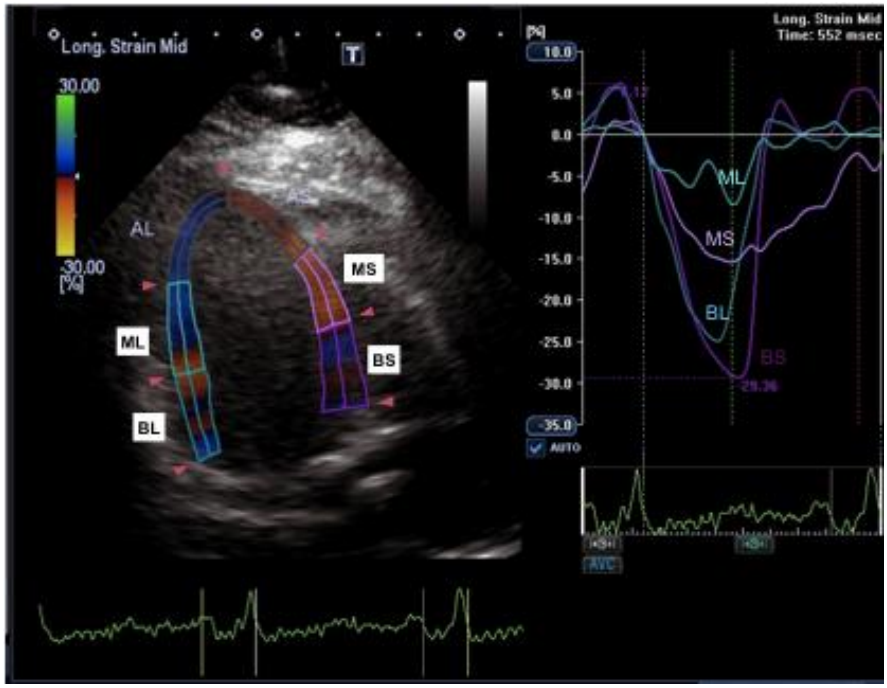

Figure 23. Longitudinal strain tracking and curves by speckle tracking echocardiography in a patient with constrictive pericarditis. BS: basal septum, MS: mid septum, BL: basal lateral, ML: mid lateral.

DOI:10.14753/SE.2012.1723

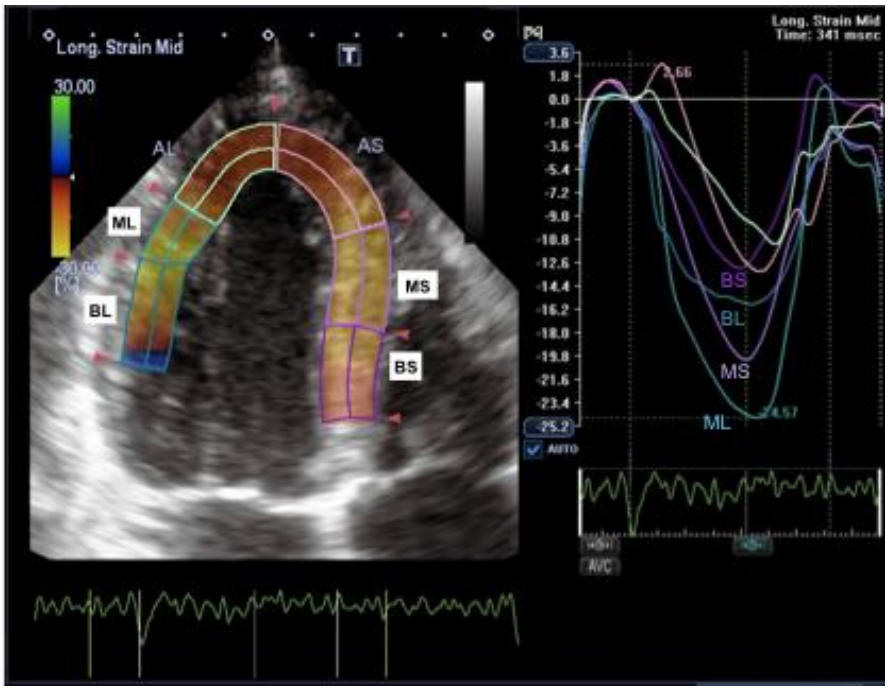

Figure 24. Longitudinal strain tracking and curves in a control subject. BS: basal septum, MS: mid septum, BL: basal lateral, ML: mid lateral.

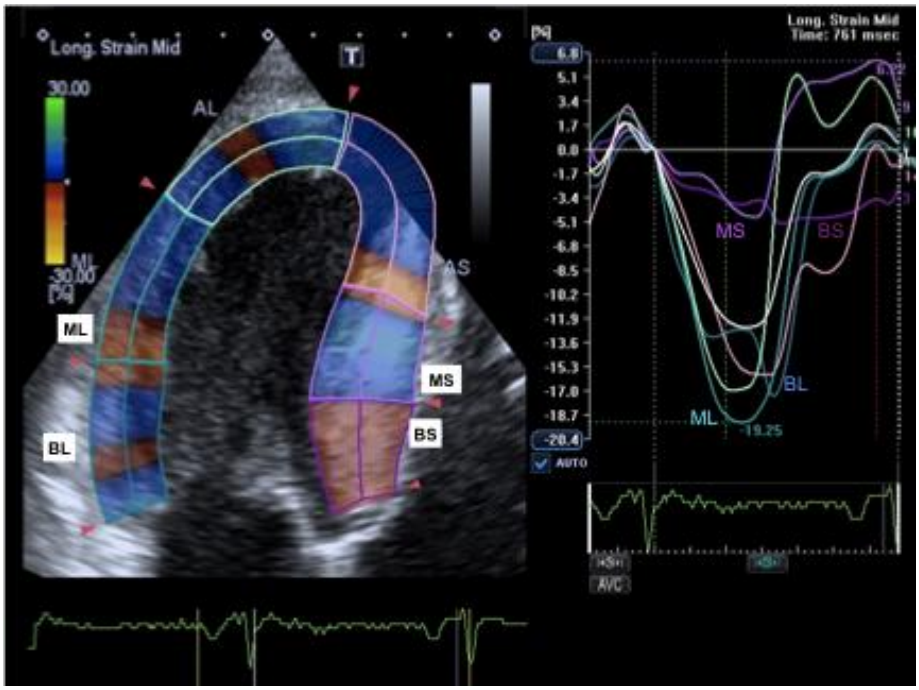

Figure 25. Longitudinal strain tracking and curves of a cardiac amyloid patient. BS: basal septum, MS: mid septum, BL: basal lateral, ML: mid lateral.

Limitations. One of the limitation of the present study is its small population, rooten in the fact that CP is a rare disease.

In CP with calcifications there were suboptimal echocardiographic images, therefore the strain analysis was very time consuming. We only used apical 4-chamber view and analyzed the longitudinal strain.

The control group was not age matched to the CP or CA group, however the main focus was to compare the two disease states, between which there was no significant difference. The RCM group consisted only cardiac amyloid patients, it would be interesting to compare CP patients with other RCM patients of other etiologies.

The important finding described in the study during endomyocardial biopsy is the development of acute thrombus related either to the sheath or to the bioptome. This complication occurred in 4% of echocardiographic guided EMB procedures overall and in 5.2% of transplant surveillance procedures and 7.1% of procedures performed to diagnose cardiac amyloid. It occurred most frequently in patients having the procedure performed via a femoral approach using a Mullins sheath. Nevertheless, thrombus formation also occurred from a trans-jugular approach. Although no overt clinical sequelae were observed in these patients (possibly in part related to prompt recognition and treatment) it is uncertain what clinical consequence unrecognized thrombus formation and thromboembolism has, especially if this complication occurs repeatedly in the same patient. This may be particularly important in cardiac transplant patients undergoing repeated surveillance biopsies using fluoroscopic guidance only and may result in progressive pulmonary hypertension, right heart failure and worsening tricuspid regurgitation. Another interesting finding was the high frequency of prior thrombosis in these patients (4 of 7 patients), one of whom had a confirmed clotting diathesis, raising the suspicion that certain patients may be more prone to this complication. Furthermore, changes to the current practice of endomyocardial biopsy seem appropriate including consideration of routine echocardiographic guidance regardless of duration post transplant, as well as continuous flushing of the sheath during the procedure.

Based on published reports, endomyocardial biopsy has a low complication rate, <1% in a Stanford series of approximately 4000 biopsies and 1,55% in a European study of 3097 biopsies.[93] Worldwide complication rates of 1.17% in 6739 procedures and 1.67%

in 2337 procedures have been reported.[94] Deckers et al [95] reported an overall complication rate of 6% in 546 procedures in adult patients with cardiomyopathy. Recently Holzmann et al reported very low major complications in both retrospective and prospective trials (0.12% versus 0%) analyzing 3048 diagnostic procedures over an 11 year period.[96] Most frequently complications relate to the manipulation of the bioptome in the heart, such as catheter induced supraventricular and ventricular arrhythmias, bradyarrhythmias, such as atrioventricular block accompanied by hemodynamic instability. Other complications relate to inadvertent trauma resulting in arterial puncture with bleeding or hematoma formation, pneumothorax, and infection. Vasovagal reactions are also observed. The most serious complications however are cardiac perforation, pericardial tamponade and death. Interestingly, in all of these studies intra-procedural thrombus formation was not identified or mentioned. Moreover, we have been unable to find prior reports of this complication of EMB in the literature.

It is interesting to speculate why this complication has not been reported before. Factors that could account for this include better image quality due to improvements in echocardiographic technology and transducer design – nevertheless, even with less sophisticated equipment it is unlikely that thrombi of this size would be missed. Other potential factors include: institutional differences in performance of the EMB procedure, and different patient mix regarding potential thrombophilic comorbidities – most procedures in this study were performed for transplant rejection surveillance. Furthermore, we think the most likely explanation for this novel observation is heightened vigilance largely due to a dedicated core group of sonographers and echocardiographers familiar with this complication. Not only do they guide the bioptome tip but they also perform repeated imaging of the sheath tip, tricuspid valve and pericardial space immediately before and after each successive biopsy. Supporting this hypothesis of increased awareness, Milner et al noted that acute thrombi were identified during percutaneous balloon mitral valvuloplasty in more than 50% of patients when imagers were specifically looking for the phenomenon.[97]

Since 2008 an interventional imaging service with eight specially trained sonographers and thirteen consultant echocardiographers was developed at Mayo Clinic, who provide echocardiographic imaging in the cardiac catheterization and electrophysiology laboratories. We have found that having a dedicated team provides more consistent

service, an appreciation of the limitations of a tomographic imaging technique while guiding catheter-based interventions and an improved level of sonographer comfort working in the sometimes stressful interventional environment. In addition, identification of infrequent complications is another example of the benefits of this initiative. These complications may otherwise have been under appreciated by a more diverse group because of their infrequent nature. The observation of acute thrombus development during EMB highlights this.

Currently, at Mayo Clinic, echocardiography is used as a supplemental imaging modality to guide EMB in patients undergoing EMB to diagnose infiltrative conditions or who are undergoing surveillance biopsies who are less than 3 month post transplant. The rationale for this has been that in non-transplant hearts as well as in the early post transplant period the risk for cardiac perforation and tamponade is greatest. Patients who undergo biopsies beyond 3 months post transplant usually have the procedure performed under fluoroscopic guidance alone. Ancillary echocardiographic imaging does have advantages regardless of the clinical setting allowing more precise positioning of the bioptome tip and avoiding inadvertent trauma to structures such as the tricuspid valve and subvalvular apparatus. It also provides prompt recognition of complications such as cardiac perforation, pericardial effusion and tamponade permitting timely management of these complications.[98] Another advantage, illustrated by this study, is the identification of thrombus formation during the procedure. The ultrasound imaging in our cases helped to make an early diagnosis and to initiate adequate therapy in order to prevent continued thrombus growth and the development of more serious pulmonary thromboembolism.

It is also interesting to speculate why thrombi developed in these seven patients. Much like the observation of catheter related thrombi during left sided chamber ablation procedures (a complication only recognized with the advent of intracardiac echocardiography) thrombi may develop within the vascular sheath when the bioptome is withdrawn and liberated on reinsertion of the bioptome on subsequent biopsies. Furthermore, a prothrombotic state may be induced by necrosis of myocytes, infiltration of mononuclear cells and release of tissue factor around the biopsy site at the time of EMB. Systemic anticoagulation is generally avoided during these procedures because of the inherent risk of bleeding. Finally, a specific clotting diathesis (as identified in one

patient) may be another contributing factor. There was no clear association between number of biopsy specimens obtained and risk of thrombus.

Finally, does thrombus formation during the procedure even matter? In the eight cases described in this study, the thrombi were promptly identified and treatment was instituted without overt clinical sequelae. Judging by the lack of prior reports of this complication, other investigators have neither seen thrombi during biopsy nor reported embolic complications. If pulmonary thromboembolism occurs it may initially go clinically unnoticed since most of the thrombi are relatively small. If however, thromboembolism occurs repeatedly, there may be clinical consequences. For example, if biopsies are done repeatedly for cardiac transplant surveillance recurrent small pulmonary thromboembolic events may potentially contribute to pulmonary hypertension and functional tricuspid regurgitation. Certainly, in instances when thrombi are large and left untreated significant pulmonary thromboembolism is likely to occur. Since this has not been previously reported, rather than not occurring, this complication may have simply been under appreciated until now.

Limitations. There are some limitations to this study. Since this is a retrospective review, it is possible that the prevalence of acute thrombus development during EMB may be an underestimation. Early on in the interventional imaging service, before cases of thrombus were identified, imagers were not specifically looking out for this complication. As we became more aware of the problem, heightened vigilance may have altered our detection rate. In addition, image resolution with transthoracic echocardiography is inferior to transesophageal echocardiography. It is known that transesophageal echocardiography is superior to transthoracic echocardiography in detecting small thrombi and thus small thrombi may have been missed in our study. Clinically this may not be important because the clot burden in these situations would likely be insignificant. Another limitation is that risk of thrombus formation may be different in patients undergoing echocardiographically guided EMB versus non-echocardiographically guided EMB. All patients included in this study underwent echo guided endomyocardial biopsy and if they were transplant recipients were thus usually less than three months post-transplant. This group may be different from transplant patients undergoing EMB who are greater than 3 months post transplant. Thus, it is not

clear that the risk of thrombus formation is the same in both echocardiographically guided and non-echocardiographically guided groups.

To the best of our knowledge, ours is the first investigation to obtain SMI measurements of all 18 LV segments in patients with iLVNC with normal and abnormal ejection fractions, and to compare these measurements to SMI measurements from healthy subjects. The main findings of the current investigation are as follows: 1) LV function, as assessed by different SMI modalities, is impaired in patients with iLVNC compared to controls, even in the group of patients with normal EF, as well as normal PWTDI e' velocity and E/e' ratio. 2) Considering systolic or diastolic longitudinal and radial/circumferential SMI modalities, the measurements with the highest diagnostic accuracy to discriminate between patients with iLVNC and normal EF and healthy subjects, are both the longitudinal sS global mean of 18 LV segments and the longitudinal sS mean of the six apical segments. 3) Consistent with peak SMI values, LV rotation/torsion values are abnormally reduced in iLVNC patients with normal EF compared to controls. Of these, the LV rotation mean of the six apical segments, LV torsion and torsion rate have the highest diagnostic accuracy, comparable to the longitudinal sS global average or the mean of the six apical segments.

Lofiego *et al*. have already reported that LV function in patients with asymptomatic iLVNC was not accompanied by less extensive non-compaction, suggesting that non-compaction is probably not the cause of LV dysfunction but rather a marker of an underlying diffuse cardiomyopathy.[99] We have confirmed this finding showing the ratio of compacted over non-compacted segments to be no different between groups II and III. Murphy and coworkers have shown that there is a long preclinical phase of disease during which patients have no symptoms or are pauci-symptomatic.[100] Therefore, it becomes critical to study whether or not there is early LV myocardial impairment in iLVNC, for diagnostic as well as potential prognostic purposes. MacMahon et al. have reported that conventional PWTDI values are reduced in patients with iLVNC and low EF[101], while Tufekcioglu and co-workers have shown abnormal systolic PWTDI values in patients with iLVNC and normal EF.[102] We believe our results go a step forward by providing evidence of significant early LV systolic and diastolic impairment in iLVNC patients with normal EF (and normal PWTDI values), assessed by multiple SMI modalities, which extends beyond the apical anatomic location, thus, providing proof

that iLVNC, as currently defined, is accompanied by an underlying myopathic process that extends beyond the non-compacted tissue.

However, differently from Tufekcioglu and co-workers, in our study, PWTDI s' velocity was not reduced in patients with iLVNC and EF > 50% compared to controls. Perhaps this was due to the different LV areas where PWTDI was measured (at the medial mitral annulus in our study, at the mid posterior wall in the previous work).

Consistent with our previous observations in another diffuse cardiomyopathy[103], longitudinal sMV and dMV-E, dSR-E and circumferential SMI values, although reduced in patients with iLVNC and low EF (group III), were not useful to discriminate between iLVNC patients with EF > 50% (group II) and controls (group I). Indeed, they were neither reduced in group II nor had sufficient sensitivity for clinical purposes (as detected by ROC analysis). On the other hand, other longitudinal SMI measurements, that are sD, sSR and sS, were significantly reduced already in group II as compared to group I, and the reduction was greater in group III. It is interesting to note the higher sensitivity of sD compared to sMVI or dMV-E for the early detection of LV impairment in group II: diagnostic accuracy of longitudinal sD, specifically of the global average of 18 LV segments which was higher than longitudinal sSR and radial sS (although the difference was not significant) and close to the accuracy reached by longitudinal sS.

Among different longitudinal SMI modalities, longitudinal sS showed the highest accuracy in discriminating group II and group I. In particular the global sS average of 18 LV segments or the mean of the 6 apical segments had very similar AUCs by ROC analysis, demonstrating that both measurements are equally useful for early detection of LV dysfunction in patients with iLVNC and normal EF. Regarding longitudinal sS, we note opposite trends in sS at the basal, mid and apical LV level between patients and controls. In particular, sS of the apical segments was higher in controls compared to basal or mid sS, whereas apical and mid sS were lower than basal sS (although the difference was not significant) in both the groups of iLVNC patients.

The observation that apical sS values are more negative (i.e. higher) in healthy subjects compared to the mid and basal sS is consistent with classic studies reporting that LV apex has a greater component of radially/circumferentially than longitudinally oriented myocardial fibers compared to other LV levels.[104, 105] Although the observation that LV function as assessed by longitudinal SMI is most impaired at the apical and middle

levels was not surprising, considering the location of hypertrabeculations and the previously published studies on pathology in iLVNC[106], it is noteworthy that longitudinal sD and sS (but not longitudinal sSR or radial SMI values) showed that LV basal segments were also impaired in group II. This observation supports the heretofore mentioned hypothesis that iLVNC is not a localized disease limited to the areas of "spongy" myocardium, but rather, a diffuse cardiomyopathy affecting LV function globally and significantly earlier than symptoms of heart failure occur. This early impairment is independent of the number of non-compacted segments (indeed group II and group III had comparable ratio of non-compacted to compacted segments.

Diagnostic usefulness of LV rotation/torsion has been already shown[107] specifically in diastolic dysfunction.[74] A recent study employing a congestive heart failure canine model showed the important relationship between LV apical rotation and global LV systolic function.[108] Our study population had an impressive reduction of LV rotation of the 6 apical segments (and therefore of LV torsion) as well as of the torsion and untorsion rates, that was already present in group II. Moreover, LV rotation of the 6 apical segments, LV torsion and LV torsion rate had highest diagnostic accuracy of discriminating between group II and group I, with AUCs obtained by ROC, comparable to those defined using longitudinal sS values, suggesting that impairment of LV apex in iLVNC is significant and involves longitudinal as well as radial/circumferential function, and making these measurements of the greatest clinical usefulness.

Limitations. This study is limited by a small sample of patients with iLVNC. However, considering the rarity of this cardiomyopathy and the statistically significant results obtained, sample size was sufficient to test our hypothesis and fulfill the aims of the study. Although we did not perform cardiac biopsy on any of our patients, we used the most sensitive and specific techniques currently available (CMR and 2D echocardiography) to confirm a diagnosis of iLVNC. Further follow-up of these patients, focused on development of overt heart failure is one objective of our ongoing investigation of enrolled patients.

DOI:10.14753/SE.2012.1723

8 Conclusions

Rare cardiac disorders are often underdiagnosed or undiagnosed due to its diagnostic challenges. Development of echocardiography has made a significant contribution to the accurate and increasing diagnosis of rare cardiological disorders. New techniques help the early diagnosis and differential diagnosis of rare cardiologic diseases such as tissue Doppler imaging and speckle tracking imaging. It can also provide prognostic information and assist in the patient management. Our results proved the usefulness of newer echocardiographic techniques.

The annulus velocity study demonstrates that in patients with CP: 1) medial e' velocity is usually higher than mitral lateral e' velocity, which is a reversal of the observed relationship in normal individuals and patients with RCM, 2) all mitral and tricuspid annular velocities (e', a' and s') are higher in primary CP compared to secondary CP, and 3) all mitral and tricuspid annular velocities decrease after pericardiectomy with normalization of the mitral lateral/medial e' velocity ratio.

Clinical implications. In patients with heart failure and normal LVEF, preserved or increased medial e' velocity strongly suggests CP. The diagnosis is further supported if medial e' is higher than mitral lateral e'. With a mitral inflow profile of increased filling pressure and expiratory hepatic vein diastolic reversals as well as abnormal ventricular septal motion, CP can be diagnosed by echocardiography. This characteristic pattern of annulus velocities reverts to normal after pericardiectomy.

The study for the differential diagnosis of CP confirms the hypothesis that the longitudinal strain of the lateral wall which is in contact with diseased pericardium is lower than that of the medial segments in CP. Speckle tracking echocardiography, specifically the ratio of medial/lateral strain measurement has an incremental value in the differential diagnosis of CP from RCM.

In conclusion the EMB study reports acute thrombus formation complicating EMB and emphasizes the usefulness of echocardiography during EMB to promptly identify this potentially serious complication facilitating timely management. This complication may be mitigated by performing continuous flushing of vascular sheaths. Furthermore patients, especially with a history of prior thrombosis or clotting diathesis, should

probably undergo routine ancillary echocardiography guided EMB rather than fluoroscopic guidance alone.

In the non-compaction study, we observed that abnormalities of different SMI modalities, in particular longitudinal sD, sS and sSR, as well as LV rotation/torsion measures, are present in patients with iLVNC, even in those asymptomatic patients with preserved EF and normal conventional PWTDI measurements. These findings provide evidence of an ongoing, subclinical myopathic process related to the morphologic presence of iLVNC. Longitudinal sS and LV rotation/torsion were the most accurate SMI modalities to differentiate between these patients and controls, and thus, may serve as a the physiologic diagnostic complement to the current morphology-based diagnosis. Furthermore, SMI assessment may have important prognostic implications that have not been proved yet. We believe SMI analysis should be performed in all patients with iLVNC referred for echocardiography and should, at a minimum, include calculation of the mean sS or LV rotation of the 6 apical segments, as well as LV torsion and torsion rate. In the event that sS curves are not satisfactory for these segments, or LV rotation/torsion is not measurable, measurement of the sD global average of the 18 LV segments is a suitable second option. Further studies in larger populations are warranted.

DOI:10.14753/SE.2012.1723

9 Summary

We present the first comprehensive analysis of systolic, early and late diastolic velocities of the mitral and tricuspid annuli in a larger number of patients with constrictive pericarditis including analysis of etiological groups and post-pericardiectomial changes.

We described a previously not reported differential method for CP and RCM. We found that the differential longitudinal strain assessment by speckle tracking echocardiography can be valuable in differentiating CP from restrictive diseases. With a cut point of 1.02, the BS / BL longitudinal strain ratio with a sensitivity rate of 91% and specificity rate of 93%, it can be an additional useful method at the verification of CP and in the differential diagnosis with CA.

Using adjunctive echocardiography to guide EMB we have identified acute intracardiac thrombus formation related to the procedure - a hitherto unreported complication. This may have important clinical implications in patients undergoing routine repeated surveillance EMB post htx, particularly those with a prior history of thrombosis or clotting diathesis. We recommend that these patients should undergo routine ancillary echocardiography guided EMB rather than fluoroscopic guidance alone. Procedural echocardiography permits early recognition and treatment of this complication.

To the best of our knowledge, ours is the first investigation to obtain SMI measurements of all 18 LV segments in patients with confirmed iLVNC with normal and abnormal ejection fractions, and to compare these measurements to SMI measurements from healthy subjects. We observed that abnormalities of different SMI modalities, in particular longitudinal sD, sS and sSR, as well as LV rotation/torsion measures, are present in patients with iLVNC, even in those asymptomatic patients with preserved EF and normal conventional PWTDI measurements. These findings provide evidence of an ongoing, subclinical myopathic process related to the morphologic presence of iLVNC. Longitudinal sS and LV rotation/torsion were the most accurate SMI modalities to differentiate between these patients and controls, and thus, may serve as a the physiologic diagnostic complement to the current morphology-based diagnosis.

DOI:10.14753/SE.2012.1723

10 Összefoglalás

Nagyszámú betegen először prezentáljuk a mitralis és tricuspidalis annulus systoles, korai és késői diastoles sebességeinek átfogó analízisét CP-ben, beleértve az etiológiai alcsoportok részletes analízisét és postpericardiectomiás változásait.

Ismereteink szerint egy új, korábban nem ismertetett differenciáldiagnosztikai módszert ismertettünk a CP és RCM elkülönítésére. A speckle tracking echocardiographia a longitudinalis strain meghatározásokkal, és a basalis medialis/lateralis aránypárok alkalmazásával hasznos információt szolgáltat e két kórkép elkülönítésében.

Echocardiographia vezérelte EMB kapcsán munkacsoportunk először számolt be az eljárás kapcsán kialakuló intracardialis akut thrombusképződésről. Fontos klinikai következményei lehetnek rutin biopsziában részesülő transzplantált betegeken, különösen azoknál, akik korábban thromboembóliás betegségben szenvedtek vagy véralvadási zavarral bírnak. Ezen betegeknek echocardiographia vezérelte EMB-t ajánlunk, a fluoroscopia kizárólagos alkalmazása helyett. Az eljárás során alkalmazott echocardiographia lehetővé teszi a szövődmény korai felismerését és azonnali kezelését.

Tudomásunk szerint munkacsoportunk vizsgálta először mind a 18 bal kamrai szegmenst speckle myocardial imaginggel NCCM-ban normal és csökkent ejekciós frakciójú betegeken, és végezte el kontroll csoporttal történő összehasonlítását. Már normál ejekciós frakciójú és normál TDI paraméterekkel bíró NCCM-ban szenvedő tünetmentes betegeken is kóros SMI értékeket figyeltünk meg, különösen a longitudinalis sD, sS, sSR, és BK-i rotációs/torziós értékek tekintetében. Ezen elváltozások egy már zajló, szubklinikai, az NCCM morfológiai jelenlétével összefüggő myopathias folyamatra utalnak. A longitudinalis sS és BK-i rotációs/torziós paraméterek tudták a legpontosabban megkülönböztetni ezen betegeket a kontroll egyénektől, ezáltal diagnosztikai kiegészítő módszerként szolgálhatnak a NCCM jelenleg használt, elsősorban morfológián alapuló diagnosztikai kritériumrendszeréhez.

DOI:10.14753/SE.2012.1723

11 References

1 Dal-Bianco JP, Sengupta PP, Mookadam F, Chandrasekaran K, Tajik AJ, Khandheria BK. Role of echocardiography in the diagnosis of constrictive pericarditis. J Am Soc Echocardiogr 2009;22:24-33.

2 Talreja DR, Edwards WD, Danielson GK, Schaff HV, Tajik AJ, Tazelaar HD, Breen JF, Oh JK. Constrictive pericarditis in 26 patients with histologically normal pericardial thickness. Circulation 2003;108:1852-1857.

3 Trappe HJ, Herrmann G, Daniel WG, Frank G, Lichtlen PR. Reduced diastolic left ventricular posterior wall motion in patients with constrictive pericarditis--incidence, hemodynamic and clinical correlations. Int J Cardiol 1988;20:53-63.

4 Engel PJ, Fowler NO, Tei CW, Shah PM, Driedger HJ, Shabetai R, Harbin AD, Franch RH. M-mode echocardiography in constrictive pericarditis. J Am Coll Cardiol 1985;6:471-474.

5 Tei C, Child JS, Tanaka H, Shah PM. Atrial systolic notch on the interventricular septal echogram: an echocardiographic sign of constrictive pericarditis. J Am Coll Cardiol 1983;1:907-912.

6 Hoit BD. Management of effusive and constrictive pericardial heart disease. Circulation 2002;105:2939-2942.

7 Voelkel AG, Pietro DA, Folland ED, Fisher ML, Parisi AF. Echocardiographic features of constrictive pericarditis. Circulation 1978;58:871-875.

8 Sengupta PP, Eleid MF, Khandheria BK. Constrictive pericarditis. Circ J 2008;72:1555-1562.

9 Izumi C, Iga K, Sekiguchi K, Takahashi S, Konishi T. Usefulness of the transgastric view by transesophageal echocardiography in evaluating thickened pericardium in patients with constrictive pericarditis. J Am Soc Echocardiogr 2002;15:1004-1008.

10 Cheitlin MD, Armstrong WF, Aurigemma GP, Beller GA, Bierman FZ, Davis JL, Douglas PS, Faxon DP, Gillam LD, Kimball TR, Kussmaul WG, Pearlman AS, Philbrick JT, Rakowski H, Thys DM. ACC/AHA/ASE 2003 guideline update for the clinical application of echocardiography-summary article: a report of the American College of Cardiology/American Heart Association Task Force on Murray RD, Apperson-Hansen C, Stugaard MPractice Guidelines (ACC/AHA/ASE Committee to Update the 1997 Guidelines for the Clinical Application of Echocardiography). J Am Coll Cardiol 2003;42:954-970.

11 D'Cruz IA, Dick A, Gross, CM, Hand CR, Lalmalani GG. Abnormal left ventricular-left atrial posterior wall contour: a new two-dimensional echocardiographic sign in constrictive pericarditis. Am Heart J 1989; 118:128-132:1119.

12 Hatle LK, Appleton CP, Popp RL. Differentiation of constrictive pericarditis and restrictive cardiomyopathy by Doppler echocardiography. Circulation 1989;79:357-370.

13 Oh JK, Hatle LK, Seward JB, Danielson GK, Schaff HV, Reeder GS, Tajik AJ. Diagnostic role of Doppler echocardiography in constrictive pericarditis. J Am Coll Cardiol 1994;23:154-162.

14 Boonyaratavej S, Oh JK, Tajik AJ, Appleton CP, Seward JB. Comparison of mitral inflow and superior vena cava Doppler velocities in chronic obstructive pulmonary disease and constrictive pericarditis. Am Coll Cardiol 1998;32:2043-2048.

15 Byrd BF 3rd, Linden RW. Superior vena cava Doppler flow velocity patterns in pericardial disease. Am J Cardiol 1990;65:1464-1470.

16 Oh JK, Tajik AJ, Appleton CP, Hatle LK, Nishimura RA, Seward JB. Preload reduction to unmask the characteristic Doppler features of constrictive pericarditis. A new observation. Circulation 1997;95:796-799.

17 Klein AL, Cohen GI, Pietrolungo JF, White RD, Bailey A, Pearce GL, Stewart WJ, Salcedo EE. Differentiation of constrictive pericarditis from restrictive cardiomyopathy by Doppler transesophageal echocardiographic measurements of respiratory variations in pulmonary venous flow. J Am Coll Cardiol 1993;22:1935-1943.

18 Sun JP, Abdalla IA, Yang XS, Rajagopalan N, Stewart WJ, Garcia MJ, Thomas JD, Klein AL. Respiratory variation of mitral and pulmonary venous Doppler flow velocities in constrictive pericarditis before and after pericardiectomy. J Am Soc Echocardiogr 2001;14:1119-1126.

19 Palka P, Lange A, Fleming AD, Donnelly JE, Dutka DP, Starkey IR, Shaw TR, Sutherland GR, Fox KA. Differences in myocardial velocity gradient measured throughout the cardiac cycle in hypetrophic cardiomyopathy, athletes and hypertensive hearts. J Am Coll Cardiol 1997;30:760–768.

20 Palka P, Lange A, Donnelly JE, Nihoyannopoulos P. Differentiation between restrictive cardiomyopathy and constrictive pericarditis by early diastolic doppler myocardial velocity gradient at the posterior wall. Circulation 2000;102:655-662.

21 Sengupta PP, Mohan JC, Pandian NG. Tissue Doppler echocardiography: principles and applications. Indian Heart J 2002;54:368-378.

22 Garcia MJ, Rodriguez L, Ares M, Griffin BP, Thomas JD, Klein AL. Differentiation of constrictive pericarditis from restrictive cardiomyopathy: assessment of left ventricular diastolic velocities in longitudinal axis by Doppler tissue imaging. J Am Coll Cardiol 1996;27:108-114.

23 Rajagopalan N, Garcia MJ, Rodriguez L, Murray RD, Apperson-Hansen C, Stugaard M, Thomas JD, Klein AL. Comparison of new Doppler echocardiographic methods to differentiate constrictive pericardial heart disease and restrictive cardiomyopathy. Am J Cardiol 2001;87:86-94.

24 Ha JW, Ommen SR, Tajik AJ, Barnes ME, Ammash NM, Gertz MA, Seward JB, Oh JK. Differentiation of constrictive pericarditis from restrictive cardiomyopathy using mitral annular velocity by tissue Doppler echocardiography. Am J Cardiol 2004;94:316-319.

25 Sohn DW, Kim YJ, Kim HS, Kim KB, Park YB, Choi YS. Unique features of early diastolic mitral annulus velocity in constrictive pericarditis. J Am Soc Echocardiogr 2004;17:222-226.

26 Ha JW, Oh JK, Ommen SR, Ling LH, Tajik AJ. Diagnostic value of mitral annular velocity for constrictive pericarditis in the absence of respiratory variation in mitral inflow velocity. J Am Soc Echocardiogr 2002;15:1468-1471.

27 Sengupta PP, Mohan JC, Mehta V, Arora R, Pandian NG, Khandheria BK. Accuracy and pitfalls of early diastolic motion of the mitral annulus for diagnosing constrictive pericarditis by tissue Doppler imaging. Am J Cardiol 2005;93:886-890.

28 Arnold MF, Voigt JU, Kukulski T, Wranne B, Sutherland GR, Hatle L. Does atrioventricular ring motion always distinguish constriction from restriction? A Doppler myocardial imaging study. J Am Soc Echocardiogr 2001;14:391-395.

29 Butz T, Langer C, Scholtz W, Jategaonkar S, Bogunovic N, Horstkotte D, Faber L. Severe calcification of the lateral mitral annulus in constrictive pericarditis: a potential pitfall for the use of echocardiographic tissue Doppler imaging. Eur J Echocardiogr 2008;9:403-405.

30 Choi EY, Ha JW, Kim JM, Ahn JA, Seo HS, Lee JH, Rim SJ, Chung N. Incremental value of combining systolic mitral annular velocity and time difference between mitral inflow and diastolic mitral annular velocity to early diastolic annular velocity for differentiating constrictive pericarditis from restrictive cardiomyopathy. J Am Soc Echocardiogr 2007;20:738-743.

31 Nagueh SF, Middleton KJ, Kopelen HA, Zoghbi WA, Quiñones MA. Doppler tissue imaging: a noninvasive technique for evaluation of left ventricular

relaxation and estimation of filling pressures. J Am Coll Cardiol 1997;30:1527-1533.

32 Ommen SR, Nishimura RA, Appleton CP, Miller FA, Oh JK, Redfield MM, Tajik AJ. Clinical utility of Doppler echocardiography and tissue Doppler imaging in the estimation of left ventricular filling pressures: A comparative simultaneous Doppler-catheterization study. Circulation 2000;102:1788-1794.

33 Ha JW, Oh JK, Ling LH, Nishimura RA, Seward JB, Tajik AJ. Annulus paradoxus: transmitral flow velocity to mitral annular velocity ratio is inversely proportional to pulmonary capillary wedge pressure in patients with constrictive pericarditis. Circulation 2001;104:976-978.

34 Chahal NS, Lim TK, Jain P, Chambers JC, Kooner JS, Senior R. Normative reference values for the tissue Doppler imaging parameters of left ventricular function: a population-based study. Eur J Echocardiogr 2010;11:51-56.

35 Reuss CS, Wilansky SM, Lester SJ, Lusk JL, Grill DE, Oh JK, Tajik AJ. Using mitral 'annulus reversus' to diagnose constrictive pericarditis. Eur J Echocardiogr 2009;10:372-375.

36 Kim JS, Ha JW, Im E, Park S, Choi EY, Cho YH, Kim JM, Rim SJ, Yoon YN, Chang BC, Chung N. Effects of pericardiectomy on early diastolic mitral annular velocity in patients with constrictive pericarditis. Int J Cardiol 2009;133:18-22.

37 Bloomfield RA, Lauson HD, Cournand A, Breed ES, Richards DW. Recording of right heart pressures in normal subjects and in patients with chronic pulmonary disease and various types of cardio-circulatory disease. J Clin Invest 1946;25:639-664.

38 Vaitkus PT, Kussmaul WG. Constrictive pericarditis versus restrictive cardiomyopathy: a reappraisal and update of diagnostic criteria. Am Heart J 1991;122:1431-1441.

39 Marwick TH, Leano RL, Brown J, Sun JP, Hoffmann R, Lysyansky P, Becker M, Thomas JD. Myocardial strain measurement with 2-dimensional speckle-tracking echocardiography: definition of normal range. JACC Cardiovasc Imaging 2009;2:80-84.

40 Saito K, Okura H, Watanabe N, Hayashida A, Obase K, Imai K, Maehama T, Kawamoto T, Neishi Y, Yoshida K. Comprehensive evaluation of left ventricular strain using speckle tracking echocardiography in normal adults: comparison of three-dimensional and two-dimensional approaches. J Am Soc Echocardiogr 2009;22:1025-1030.

41 Cunningham KS, Veinot JP, Butany J. An approach to endomyocardial biopsy interpretation. J Clin Pathol 2006;59:121-129.

42 Chen RJ, Wei J, Chang CY, Lee KC, Sue SH, Chen HL. Tricuspid valve regurgitation and endomyocardial biopsy after orthotopic heart transplantation. Transplant Proc 2008;40:2603-2606.

43 Sloan KP, Bruce CJ, Oh JK, Rihal CS. Complications of echocardiography-guided endomyocardial biopsy. J Am Soc Echocardiogr 2009;22:321-324.

44 Oechslin EN, Attenhofer Jost CH, Rojas JR, Kaufmann PA, Jenni R. Long-term follow-up of 34 adults with isolated left ventricular noncompaction: a distinct cardiomyopathy with poor prognosis. J Am Coll Cardiol 2000;36:493-500.

45 Jenni R, Oechslin E N, van der Loo B. Isolated ventricular noncompaction of the myocardium in adults. Heart 2007;93:11-15.

46 Cavusoglu Y, Ata N, Timuralp B, Gorenek B, Goktekin O, Kudaiberdieva G, Unalir A. Noncompaction of the ventricular myocardium: Report of two cases with bicuspid aortic valve demonstrating poor prognosis and with prominent right ventricular involvement. Echocardiography 2003; 20:379-383.

47 Hsiao SH, Lee TY, Mar GY. Left ventricular non-compaction associated with patent ductus arteriosus. Acta Cardiol Sin 2004;20:251-255.

48 Attenhofer Jost CH, Connolly HM, Warnes CA, Warnes CA, O'leary P, Tajik AJ, Pellikka PA, Seward JB. Noncompacted myocardium in Ebstein's anomaly: initial description in three patients. J Am Soc Echocardiogr 2004; 17:677-680.

49 Rigopoulos A, Rizos IK, Aggeli C, Kloufetos P, Papacharalampous X, Stefanadis C, Toutouzas P. Isolated left ventricular noncompaction: an unclassified cardiomyopathy with severe prognosis in adults. Cardiology 2002;98:25-32.

50 Sengupta PP, Mohan JC, Mehta V, Jain V, Arora R, Pandian NG, Khandheria BK. Comparison of echocardiographic features of noncompaction of the left ventricle in adults versus idiopathic dilated cardiomyopathy in adults. Am J Cardiol 2004;94:389-391.

51 Ali SKM, Omran AS, Najm H, Godman MJ. Noncompaction of the left ventricular myocardium associated with mitral regurgitation and preserved ventricular systolic function. J Am Soc Echocardiogr 2004;17:87-89.

52 Jenni R, Oechslin E N, van der Loo B. Isolated ventricular noncompaction of the myocardium in adults. Heart 2007;93:11-15.

53 Shizukuda Y, Bhatti S, Munjal J, Hu YL, Harrelson A. Personalized echocardiography: clinical applications of advanced echocardiography and future directions. Future Cardiol 2010;6:833-844.

54 Nesbitt GC, Mankad S, Oh JK. Strain imaging in echocardiography: methods and clinical applications. Int J Cardiovasc Imaging 2009;25 Suppl 1:9-22.

55 Isaaz K, Thompson A, Ethevenot G, Cloez JL, Brembilla B, Pernot C. Doppler echocardiographic measurement of low velocity motion of the left ventricular posterior wall. Am J Cardiol 1989;64:66-75.

56 McDicken WN, Sutherland GR, Moran CM, Gordon LN. Colour Doppler velocity imaging of the myocardium. Ultrasound Med Biol 1992;18:651-654.

57 Mor-Avi V, Lang RM, Badano LP, Belohlavek M, Cardim NM, Derumeaux G, Galderisi M, Marwick T, Nagueh SF, Sengupta PP, Sicari R, Smiseth OA, Smulevitz B, Takeuchi M, Thomas JD, Vannan M, Voigt JU, Zamorano JL. Current and evolving echocardiographic techniques for the quantitative evaluation of cardiac mechanics: ASE/EAE consensus statement on methodology and indications endorsed by the Japanese Society of Echocardiography. Eur J Echocardiogr 2011;12:167-205.

58 Oh JK, Seward JB, Tajik JA. The Echo Manual. Third Edition. 2007.

59 Bellavia D. New Doppler Myocardial Imaging Techniques are useful for the early diagnosis of cardiac involvement and for risk stratification in patients with primary systemic (AL) amyloidosis. A thesis submitted to the faculty of the Mayo Clinic College of Medicine Mayo Graduate School 2008.

60 Nikitin NP, Witte KK. Application of tissue Doppler imaging in cardiology. Cardiology 2004;101:170-184.

61 Isaaz K. What are we actually measuring by Doppler tissue imaging? J Am Coll Cardiol 2000;36:897-899.

62 D'hooge J, Heimdal A, Jamal F, Kukulski T, Bijnens B, Rademakers F, Hatle L, Suetens P, Sutherland GR. Regional strain and strain rate measurements by cardiac ultrasound: principles, implementation and limitations. Eur J Echocardiogr 2000;1:154-170.

63 Chen J, Liu W, Zhang H, Lacy L, Yang X, Song SK, Wickline SA, Yu X. Regional ventricular wall thickening reflects changes in cardiac fiber and sheet structure during contraction: quantification with diffusion tensor MRI. Am J Physiol Heart Circ Physiol 2005;289:898-907.

64 Nielsen PM, Le Grice IJ, Smaill BH, Hunter PJ. Mathematical model of geometry and fibrous structure of the heart. Am J Physiol 1991;260:1365-1378.

65 Saito K, Okura H, Watanabe N, Hayashida A, Obase K, Imai K, Maehama T, Kawamoto T, Neishi Y, Yoshida K. Comprehensive evaluation of left ventricular strain using speckle tracking echocardiography in normal adults: comparison of three-dimensional and two-dimensional approaches. J Am Soc Echocardiogr 2009;22:1025-1030.

66 Amundsen BH, Helle-Valle T, Edvardsen T. Noninvasive myocardial strain measurement by speckle tracking echocardiography: validation against sonomicrometry and tagged magnetic resonance imaging. J Am Coll Cardiol 2006;47:789–793.

67 Goffinet C, Vanoverschelde JL. Speckle Tracking Echocardiography. Philips. European Cardiovascular Disease 2007.

68 Helle-Valle T, Crosby J, Edvardsen T, Lyseggen E, Amundsen BH, Smith HJ, Rosen BD, Lima JA, Torp H, Ihlen H, Smiseth OA. New noninvasive method for assessment of left ventricular rotation: speckle tracking echocardiography.Circulation 2005;112:3149–3156.

69 Notomi Y, Lysyansky P, Setser RM, Shiota T, Popović ZB, Martin-Miklovic MG, Weaver JA, Oryszak SJ, Greenberg NL, White RD, Thomas JD. Measurement of ventricular torsion by two-dimensional ultrasound speckle tracking imaging, J Am Coll Cardiol 2005;45:2034–2041.

70 Quinones MA, Pickering E, Alexander JK. Percentage of shortening of the echocardiographic left ventricular dimension. Its use in determining ejection fraction and stroke volume. Chest 1978;74:59-65.

71 Jiamsripong P, Honda T, Reuss CS, Hurst RT, Chaliki HP, Grill DE, Schneck SL, Tyler R, Khandheria BK, Lester SJ. Three methods for evaluation of left atrial volume. Eur J Echocardiogr 2008; 9:351-355.

72 Lang RM, Bierig M, Devereux RB, Flachskampf FA, Foster E, Pellikka PA, Picard MH, Roman MJ, Seward J, Shanewise JS, Solomon SD, Spencer KT, Sutton MS, Stewart WJ. Recommendations for chamber quantification: a report

from the American Society of Echocardiography's Guidelines and Standards Committee and the Chamber Quantification Writing Group, developed in conjunction with the European Association of Echocardiography, a branch of the European Society of Cardiology. J Am Soc Echocardiogr 2005;18:1440-1463.

73 Leitman M, Lysyansky P, Sidenko S, Shir V, Peleg E, Binenbaum M, Kaluski E, Krakover R, Vered Z. Two-dimensional strain-a novel software for real-time quantitative echocardiographic assessment of myocardial function. J Am Soc Echocardiogr 2004;17:1021-1029.

74 Park SJ, Miyazaki C, Bruce CJ, Ommen S, Miller FA, Oh JK. Left ventricular torsion by two-dimensional speckle tracking echocardiography in patients with diastolic dysfunction and normal ejection fraction. J Am Soc Echocardiogr 2008;21:1129-1137.

75 Mehta CR, Patel NR, Tsiatis AA. Exact significance testing for ordered categorical data. Biometrics 1984;40:819-825.

76 Shrout PE, Fleiss JL. Intraclass correlations: uses in assessing rater reliability. Psychol Bull 1979;86:420-428.

77 Garcia MJ, Rodriguez L, Ares M, Griffin BP, Thomas JD, Klein AL. Differentiation of constrictive pericarditis from restrictive cardiomyopathy: assessment of left ventricular diastolic velocities in longitudinal axis by Doppler tissue imaging. J Am Coll Cardiol 1996;27:108-114.

78 D'Cruz IA, Levinsky R, Anagnostopoulos C, Ares M, Griffin BP, Thomas JD, Klein AL. Echocardiographic diagnosis of partial pericardial constriction of the left ventricle. Radiology 1978; 127:755-756.

79 Gongora E, Dearani JA, Orszulak TA, Schaff HV, Li Z, Sundt TM 3rd. Tricuspid regurgitation in patients undergoing pericardiectomy for constrictive pericarditis. Ann Thorac Surg 2008; 85:163-170.

80 Ama R, Segers P, Roosens C, Claessens T, Verdonck P, Poelaert J. The effects of load on systolic mitral annular velocity by tissue Doppler imaging. Anaesth Analg 2004; 99:332-338.

81 Mishiro Y, Oki T, Yamada H. Evaluation of left ventricular contraction abnormalities in patients with dilated cardiomyopathy with the use of pulsed tissue Doppler imaging. J Am Soc Echocardiogr 1999; 12:913-920.

82 Yamahada H, Oki T, Tabata T. Assessment of left ventricular systolic wall motion velocity with pulsed tissue Doppler imaging: comparison with peak dP/dt of the left ventricular pressure curve. J Am Soc Echocardiogr 1998;11:442-449.

83 Alam M, Wardell J, Andersson E, Samad BA, Nordlander R. Effects of first myocardial infarction on left ventricular systolic and diastolic function with the use of mitral annular velocity determinded by pulsed wave doppler tissue imaging. J Am Soc Echocardiogr 2000; 13:343-352.

84 Homsi M, Mahenthiran J, Vaz D, Sawada SG. Reduced right ventricular systolic function in constrictive pericarditis indicates myocardial involvement and persistent right ventricular dysfunction and symptoms after pericardiectomy. J Am Soc Echocardiogr 2007; 20:1417.-1-7.

85 Ohte N, Narita H, Hashimoto T, Akita S, Kurokawa K, Fujinami T. Evaluation of left ventricular early diastolic performance by color tissue Doppler imaging of the mitral annulus. Am J Cardiol 1998; 82:1414-1417.

86 Masui T, Finck S, Higgins CB. Constrictive pericarditis and restrictive cardiomyopathy: evaluation with MR imaging. Radiology 1992; 182:369-73.

87 Sengupta PP, Krishnamoorthy VK, Abhayaratna WP, Korinek J, Belohlavek M, Sundt TM 3rd, Chandrasekaran K, Mookadam F, Seward JB, Tajik AJ, Khandheria BK. Disparate patterns of left ventricular mechanics differentiate constrictive pericarditis from restrictive cardiomyopathy. JACC Cardiovasc Imaging 2008;1:29-38.

88 Li Y, Garson CD, Xu Y, Beyers RJ, Epstein FH, French BA, Hossack JA. Quantification and MRI validation of regional contractile dysfunction in mice post myocardial infarction using high resolution ultrasound. Ultrasound Med Biol 2007;33:894-904.

89 Cho GY, Chan J, Leano R, Strudwick M, Marwick TH. Comparison of two-dimensional speckle and tissue velocity based strain and validation with harmonic phase magnetic resonance imaging. Am J Cardiol 2006;97:1661-1666.

90 Korinek J, Wang J, Sengupta PP, Miyazaki C, Kjaergaard J, McMahon E, Abraham TP, Belohlavek M. Two-dimensional strain--a Doppler-independent ultrasound method for quantitation of regional deformation: validation in vitro and in vivo. J Am Soc Echocardiogr 2005;18:1247-1253.

91 Korinek J, Kjaergaard J, Sengupta PP, Yoshifuku S, McMahon EM, Cha SS, Khandheria BK, Belohlavek M. High spatial resolution speckle tracking improves accuracy of 2-dimensional strain measurements: an update on a new method in functional echocardiography. J Am Soc Echocardiogr 2007;20:165-170.

92 Sengupta P, Eleid MF, Sundt TM. Regional variability of pericardial thickness influences left ventricular diastolic recoil mechanics in constrictive pericarditis. J Am Soc Echocardiogr 2008; 21:518.

93 Fowles RE, Mason JW. Endomyocardial biopsy. Ann Intern Med 1982;97:885-894.

94 Richardson PJ. Technique of endomyocardial biopsy--including a description of a new form of endomyocardial bioptome. Postgrad Med J 1975;51:282-285.

95 Deckers JW, Hare JM, Baughman KL. Complications of transvenous right ventricular endomyocardial biopsy in adult patients with cardiomyopathy: a seven-year survey of 546 consecutive diagnostic procedures in a tertiary referral center. J Am Coll Cardiol 1992;19:43-47.

96 Holzmann M, Nicko A, Kuhl U, Noutsias M, Poller W, Hoffmann W, Morguet A, Witzenbichler B, Tschöpe C, Schultheiss HP, Pauschinger M. Complication rate of right ventricular endomyocardial biopsy via the femoral approach: a retrospective and prospective study analyzing 3048 diagnostic procedures over an 11-year period. Circulation 2008;118:1722-1728.

97 Milner MR, Goldstein SA, Pichard AD. Transesophageal echocardiographic detection of transseptal catheter-related thrombi in patients with mitral stenosis. JACC 1991;17:261A abstract.

98 Drury JH, Labovitz AJ, Miller LW. Echocardiographic Guidance for Endomyocardial Biopsy. Echocardiography 1997;14:469-474.

99 Lofiego C, Biagini E, Pasquale F, Ferlito M, Rocchi G, Perugini E, Bacchi-Reggiani L, Boriani G, Leone O, Caliskan K, ten Cate FJ, Picchio FM, Branzi A, Rapezzi C. Wide spectrum of presentation and variable outcomes of isolated left ventricular non-compaction. Heart 2007;93: 65-71.

100 Murphy RT, Thaman R, Blanes JG, Ward D, Sevdalis E, Papra E, Kiotsekoglou A, Tome MT, Pellerin D, McKenna WJ, Elliott PM. Natural history and familial characteristics of isolated left ventricular non-compaction. Eur Heart J 2005;26:187-192.

101 McMahon CJ, Pignatelli RH, Nagueh SF, Lee VV, Vaughn W, Valdes SO, Kovalchin JP, Jefferies JL, Dreyer WJ, Denfield SW, Clunie S, Towbin JA, Eidem BW. Left ventricular non-compaction cardiomyopathy in children: characterisation of clinical status using tissue Doppler-derived indices of left ventricular diastolic relaxation. Heart 2007;93:676-81.

102 Tufekcioglu O, Aras D, Yildiz A, Topaloglu S, Maden O. Myocardial contraction properties along the long and short axes of the left ventricle in isolated left ventricular non-compaction: pulsed tissue Doppler echocardiography. Eur J Echocardiogr 2008;9:344-350.

103 Bellavia D, Pellikka PA, Abraham TP, Al-Zahrani GB, Dispenzieri A, Oh JK, Bailey KR, Wood CM, Lacy MQ, Miyazaki C, Miller FA Jr. Evidence of impaired left ventricular systolic function by Doppler myocardial imaging in patients with systemic amyloidosis and no evidence of cardiac involvement by standard two-dimensional and Doppler echocardiography. Am J Cardiol 2008;101:1039-1045.

104 Kowalski M, Kukulski T, Jamal F, D'hooge J, Weidemann F, Rademakers F, Bijnens B, Hatle L, Sutherland GR. Can natural strain and strain rate quantify regional myocardial deformation? A study in healthy subjects. Ultrasound Med Biol2001;27:1087-1097.

105 Andersen NH, Poulsen SH. Evaluation of the longitudinal contraction of the left ventricle in normal subjects by Doppler tissue tracking and strain rate. J Am Soc Echocardiogr 2003;16:716-723.

106 Burke A, Mont E, Kutys R, Virmani R. Left ventricular noncompaction: a pathological study of 14 cases. Hum Pathol 2005;36:403-411.

107 Sengupta PP, Krishnamoorthy VK, Korinek J, Narula J, Vannan MA, Lester SJ, Tajik JA, Seward JB, Khandheria BK, Belohlavek M. Left ventricular form and function revisited: applied translational science to cardiovascular ultrasound imaging. J Am Soc Echocardiogr 2007;20:539-551.

108 Wang J, Nagueh SF, Mathuria NS, Shih HT, Panescu D, Khoury DS. Left ventricular twist mechanics in a canine model of reversible congestive heart failure: a pilot study. J Am Soc Echocardiogr 2009;22:95-98.

DOI:10.14753/SE.2012.1723

12 Publications

12.1 Publications related to the thesis

Veress G, Bruce CJ, Kutzke K, Click RL, Scott CG, Oh JK, Rihal CS. Acute thrombus formation as a complication of right ventricular biopsy. J Am Soc Echocardiogr 2010;23:1039-1044.

IF: 3.518

Bellavia D, Michelena HI, Martinez M, Pellikka PA, Bruce CJ, Connolly HM, Villarraga HR, **Veress G**, Oh JK, Miller FA. Speckle myocardial imaging modalities for early detection of myocardial impairment in isolated left ventricular non-compaction. Heart 2010;96:440-447.

IF: 4.706

Veress G, Ling LH, Kim KH, Dal-Bianco JP, Schaff HV, Espinosa RE, Melduni RM, Tajik AJ, Sundt TM, III, Oh JK. Mitral and tricuspid annular velocities before and after pericardiectomy in patients with constrictive pericarditis. Circ Cardiovasc Imaging 2011;4:399-407.

IF: 4.757 (2010)

Veress G, Apor A, Merkely B. Constrictive pericarditis nowadays. Cardiol Hung 2011:41;263-268.

Veress G, Kim KH, Masaki M, Espinosa RE, Oh JK. Differential diagnosis of constrictive pericarditis from restrictive myocardial disease by speckle tracking echocardiography. J Am Coll Cardiol (Suppl A) 2010;55:10.

IF: 14.292

Veress G, Kim KH, Masaki M, Espinosa RE, Apor A, Merkely B, Oh JK. Speckle tracking echokardiográfia mint egy új diagnosztikai módszer a konstriktív pericarditis és restriktív cardiomyopathia elkülönítésére. Cardiol Hung 2010;40:G9.

Veress G, Apor A, Ling LH, Kim KH, Schaff H, Espinosa RE, Tajik JA, Sundth TM, Merkely B, Oh JK. Mitral and tricuspid annular velocities before and after pericardiectomy in patients with constrictive pericarditis. Cardiol Hung 2011;41:F8.

12.2 Other publications and citable abstracts

Masaki M, Yuasa T, Cha YM, **Veress G**, Dong K, Mankad SV, Oh JK. 2D ultrasound speckle tracking strain imaging of the left atrium in the estimation of left ventricular filling pressures. J Am Coll Cardiol (Suppl A) 2010;55:10.
IF:14.292

Veress G, Vago H, Apor A, Barta E, Szelid Zs, Toth L, Varju I, Szabolcs Z, Merkely B. Kettős lokalizációjú primer szívtumor – esetismertetés. Cardiol Hung (Suppl B) 2008; p. B75.

Kutyifa V, Veress G, Apor A, Andrassy P, Szilagyi Sz, Geller L Merkely B. Szöveti Doppler echocardiographia szerepe cardialis resyncronisatios terápia során. Cardiol Hung (Suppl B) 2008; p. B60

Veress G, Merkely B, Masszi J, Gellér L, Faluközy J, Kutyifa V, **Veress G Jr,** Mikes G, Simon A, Berényi I. Early results of comprehensive cardiac rehabilitation after biventricular pacemaker implantation. Eur J Cardiovasc Prev Rehabil 2007; 92: 363.
IF: 2.221

Veress G, Merkely B, Masszi J, Faluközy J, Dobrán I, Simon A, **Veress G Jr**. The rehabilitation of patients with biventricular pacemakers. Cardiol Hung 2005; 35: B3.

Tihanyi L, Veress G Jr, Simon A, Veress G. A pericardiumot érintő korai és késői szövődmények szívműtét után – 9 éves retrospektív vizsgálat alapján. Kardiovaszkuláris prevenció és rehabilitáció 2011; 3: 24-26.

Impact factor of original papers: 12.981

Impact factor of citable abstracts: 30.80

DOI:10.14753/SE.2012.1723

13 Acknowledgement

First of all I would like to acknowledge and thank to my PhD supervisor and Cardiology Professor Béla Merkely MD, PhD, DSc for his constant, outstanding guidance and support during the entire PhD program.

Similarly, I would like to thank to Professor Jae K Oh, MD, who was my mentor during my one year research fellowship and consecutive one year research collaboration in the Echocardiography Laboratory at Mayo Clinic, in Rochester, MN. I am grateful in every possible way for his constructive and valuable leadership during my stay.

My consultant colleagues warrant special mention and thanks for their insightful and detailed suggestions, which helped my research work to a great extent. They were Astrid Apor MD, Kim Kyehun MD, PhD, Lieng H Ling MD, Bellavia Diego, MD, PhD, Masaki Mitsuru, MD and all of my co-authors with our scientific papers.

Collective and individual acknowledgements are also owed to all my colleagues, in particular to Elektra Bartha MD, Nagy Andrea MD, PhD, Zsolt Szelíd MD, PhD, Krisztina Heltai MD, PhD, Kékesi Violetta MD, PhD and Dávid Becker MD, PhD furthermore to sonographers, assistants and statisticians at Semmelweis University Heart Center and Mayo Clinic, Echo Lab. Many thanks go to Melinda Sarusi, secretary at the Semmelweis University Heart Center for her assistance.

Finally, I wish to thank my family for their exceptional support and encouragement.